

# A Versatile Pilot Design Scheme for FDD Systems Utilizing Gaussian Mixture Models

Nurettin Turan, *Graduate Student Member, IEEE*, Benedikt Böck, *Graduate Student Member, IEEE*,  
 Benedikt Fesl, *Graduate Student Member, IEEE*, Michael Joham, *Member, IEEE*,  
 Deniz Gündüz, *Fellow, IEEE*, and Wolfgang Utschick, *Fellow, IEEE*

**Abstract**—In this work, we propose a Gaussian mixture model (GMM)-based pilot design scheme for downlink (DL) channel estimation in single- and multi-user multiple-input multiple-output (MIMO) frequency division duplex (FDD) systems. In an initial offline phase, the GMM captures prior information during training, which is then utilized for pilot design. In the single-user case, the GMM is utilized to construct a codebook of pilot matrices and, once shared with the mobile terminal (MT), can be employed to determine a feedback index at the MT. This index selects a pilot matrix from the constructed codebook, eliminating the need for online pilot optimization. We further establish a sum conditional mutual information (CMI)-based pilot optimization framework for multi-user MIMO (MU-MIMO) systems. Based on the established framework, we utilize the GMM for pilot matrix design in MU-MIMO systems. The analytic representation of the GMM enables the adaptation to any signal-to-noise ratio (SNR) level and pilot configuration without re-training. Additionally, an adaption to any number of MTs is facilitated. Extensive simulations demonstrate the superior performance of the proposed pilot design scheme compared to state-of-the-art approaches. The performance gains can be exploited, e.g., to deploy systems with fewer pilots.

**Index Terms**—Pilot design, Gaussian mixture models, machine learning, MU-MIMO, FDD systems.

## I. INTRODUCTION

In MIMO communication systems, obtaining channel state information (CSI) at the base station (BS) needs to occur in regular time intervals. In FDD systems, both the BS and the MTs transmit at the same time but on different frequencies, which breaks the reciprocity between the instantaneous uplink (UL) CSI and DL CSI. Consequently, acquiring DL CSI at the BS in FDD systems is challenging [2] and, thus, relies on feedback of the estimated channels from the MTs rendering the quality of DL channel estimation critically important.

However, the channel estimation quality is strongly influenced by the choice of pilots, demonstrating the need for sophisticated pilot design schemes in FDD systems. In massive MIMO systems, where the BS is typically equipped with a high

number of antennas, as many pilots as transmit antennas are required to be sent from the BS to the MT to fully illuminate the channel, i.e., avoiding a systematic error when relying on least squares (LS) DL CSI estimation at the MT. However, the associated pilot overhead for complete channel illumination can be prohibitive [3]. In scenarios with spatial correlation at the BS and the MTs, the DL training overhead can be significantly reduced by leveraging statistical knowledge of the channel and the noise [4]–[11], e.g., by using Bayesian estimation approaches in combination with well-designed pilot matrices according to different optimization criteria.

In particular, in [4]–[7], the single-user case is analyzed, where [4] considers a multiple-input single-output (MISO) system and in [5]–[7], a MIMO setup with a Kronecker correlation model is investigated. These works consider the minimization of the mean squared error (MSE) as the optimization criterion for DL channel estimation. A common approach is to send the eigenvectors of the transmit-side covariance matrix corresponding to the strongest eigenvalues as pilots. Further, considering different power levels allows to adaptively scale these pilot vectors following a water-filling procedure. So-called unitary pilots, i.e., assigning equal power to each pilot vector, can also be used for practical reasons [4]. In [8]–[11], multi-user MISO (MU-MISO) setups, are considered. The work [8] considers minimizing the sum of MSEs associated with the channel estimate of all MTs, whereas [10] considers minimizing the weighted sum MSE. Using the close relationship between the mutual information and the MSE [12], the work [9] considers maximizing the sum CMI expression to design the pilot matrix. In [11], the channels are assumed to be distributed according to a Gaussian mixture distribution, and mutual information maximization is adopted. The works [9]–[11] apply iterative algorithms for designing the pilot matrices. However, all of the aforementioned works rely on either perfect or estimated statistical knowledge at the BS and/or at the MTs' side, which may be difficult to acquire.

In this context, the recent works in [13], [14] propose machine learning-based frameworks for combining the pilot matrix design with DL channel estimation. In particular, end-to-end deep neural networks (DNNs) are employed to jointly learn a pilot matrix and a channel estimation module. In this way, the designed pilots are optimized for the whole scenario, i.e., a global pilot matrix is learned offline and remains fixed for channel estimation in the online phase. However, these end-to-end DNNs cannot provide MT-adaptive pilot matrices, neither for the single-user case nor the multi-user case, since

Preliminary results have been presented at ISWCS'24 [1].

The authors acknowledge the financial support by the Federal Ministry of Education and Research of Germany in the program of “Souverän. Digital. Vernetzt.”. Joint project 6G-life, project identification number: 16KISK002.

N. Turan, B. Böck, B. Fesl, M. Joham, and W. Utschick are with the TUM School of Computation, Information and Technology, Technische Universität München, 80333 Munich, Germany (e-mail: nurettin.turan@tum.de; benedikt.boeck@tum.de; benedikt.fesl@tum.de; joham@tum.de; utschick@tum.de).

D. Gündüz is with the Department of Electrical and Electronic Engineering, Imperial College London, London SW7 2AZ, U.K. (e-mail: d.gunduz@imperial.ac.uk).

©This work has been submitted to the IEEE for possible publication. Copyright may be transferred without notice, after which this version may no longer be accessible.

knowledge about MT-specific statistics, which could be inferred in the online phase, can not be leveraged. In other words, with the above-mentioned end-to-end DNNs, pilot matrices tailored for a specific MT or a constellation of multiple MTs are not possible. Moreover, end-to-end DNNs are inflexible regarding the number of pilots, since different numbers of pilots require a pilot matrix of suitable dimension and a dedicated channel estimation module, i.e., several end-to-end DNNs are required. The SNR level-specific training further hinders practicability.

In recent years, generative models have been utilized for wireless communications entities. Generally, generative models refer to techniques that aim to learn the underlying distribution of a training data set and provide a prior for different applications. Generative concepts such as generative adversarial networks [15], variational autoencoders [16], and diffusion models [17] gained significant attention. In wireless communications, these generative models have been applied to channel estimation [18], to precoding [19], and as channel modeling frameworks, e.g., [20], [21]. In this work, we utilize GMMs, which are widely adopted in wireless communications research. For instance, GMMs are employed for predicting channel states in [22], for multi-path clustering in [23], and for pilot optimization in [24]. Note that a fundamental difference of our work to [24] is that we do not assume that the true channel probability density function (PDF) is given and is equal to a Gaussian mixture distribution. More recently, GMMs were used for channel estimation in [25], for channel prediction in scenarios with high mobility in [26], and were leveraged to design a feedback scheme for precoding in single- and multi-user systems in [27]. The universal approximation ability of GMMs, cf. [28], justifies the strong performance in the above-mentioned applications. Beyond this ability, the primary motivation for leveraging GMMs in this work to propose a versatile pilot design scheme for point-to-point MIMO and MU-MIMO FDD systems is the following. GMMs are generative models that comprise a discrete latent space. This characteristic makes the inference of the latent variable, given an observation, particularly tractable.

The contributions of this work are summarized as follows:

- 1) The proposed GMM-based pilot design scheme neither requires *a priori* knowledge of the channel's statistics at the BS nor the MT. The statistical prior information captured by the GMM in the initial offline phase is exploited to determine a feedback index at the MT, encoded by  $B$  bits. This feedback index is sufficient to establish common knowledge of the pilot matrix, which is selected from a codebook of pilot matrices. Thus, no online pilot optimization is required in the single-user case.
- 2) The sum CMI-based multi-user pilot optimization framework from [9] only considers single antenna MTs. However, with trends towards massive MIMO, both the BS and the MTs are equipped with many antennas [29]. In this work, we extend the sum CMI maximization to MU-MIMO systems, i.e., the MTs are also equipped with multiple antennas. Additionally, we establish a lower bound to the sum CMI in a MU-MIMO system and discuss conditions when the lower bound is equal to the

sum CMI or exhibits the largest gap to the sum CMI. We further recognize that the maximization of the lower bound involves the usage of the iterative algorithm from [9] and provides complexity savings in the online pilot matrix optimization.

- 3) Based on the extension of the sum CMI framework, we utilize the GMM-based scheme for pilot matrix design in MU-MIMO systems. Again, no *a priori* statistical knowledge is required. In the multi-user case, each MT determines its  $B$  bits feedback information and transfers it back to the BS. Using a feedforward link, the BS broadcasts the collected feedback indices to all MTs. The pilot matrix is then found using the respective GMM-component's covariance. Due to the quantized information associated with the component selection of the GMM, the proposed scheme offers significant gains over state-of-the-art feedforward signaling schemes, which quantizes the pilot matrix after optimization.
- 4) The analytic representation of the GMM generally allows the adaption to any SNR level and pilot configuration without re-training. In the multi-user case, an adaption to any number of MTs is facilitated. Moreover, the GMM's so-called responsibilities that are needed for inferring the feedback index can be further processed to a channel estimate at the MTs. Based on extensive simulations, we highlight the superior performance of the proposed scheme compared to state-of-the-art approaches. The gains can be exploited, e.g., to deploy systems with fewer pilots.

*Notation:* Matrices and vectors are denoted with bold uppercase and bold lowercase letters, respectively. The transpose, conjugate, and conjugate transpose of a matrix  $\mathbf{A}$  is denoted by  $\mathbf{A}^T$ ,  $\mathbf{A}^*$ , and  $\mathbf{A}^H$ , respectively. The all-zeros vector and the identity matrix with appropriate dimensions are denoted by  $\mathbf{0}$  or  $\mathbf{I}$ , respectively. The canonical unit vector that contains a one at the  $i$ -th entry and is zero elsewhere is denoted by  $\mathbf{e}_i$ . The Euclidean norm of a vector  $\mathbf{a} \in \mathbb{C}^N$  is denoted by  $\|\mathbf{a}\|$ . A complex-valued normal distribution with mean vector  $\boldsymbol{\mu}$  and covariance matrix  $\mathbf{C}$  is denoted by  $\mathcal{N}_{\mathbb{C}}(\boldsymbol{\mu}, \mathbf{C})$  and  $\sim$  stands for "distributed as." The determinant, the rank, and the trace of matrix  $\mathbf{A}$  is given by  $\det(\mathbf{A})$ ,  $\text{rk}(\mathbf{A})$ , and  $\text{tr}(\mathbf{A})$ , respectively. The vectorization (stacking columns) of a matrix  $\mathbf{A} \in \mathbb{C}^{m \times N}$  is written as  $\mathbf{a} = \text{vec}(\mathbf{A}) \in \mathbb{C}^{mN}$ , and the reverse operation is denoted by  $\mathbf{A} = \text{unvec}_{m,N}(\mathbf{a})$ . The vector of the diagonal elements of a diagonal matrix  $\mathbf{A}$  is denoted by  $\text{diag}(\mathbf{A})$ , and the diagonal matrix with a vector  $\mathbf{a}$  on its diagonal is denoted by  $\text{diag}(\mathbf{a})$ . The Kronecker product of two matrices  $\mathbf{A} \in \mathbb{C}^{m_1 \times N_1}$  and  $\mathbf{B} \in \mathbb{C}^{m_2 \times N_2}$  is  $\mathbf{A} \otimes \mathbf{B} \in \mathbb{C}^{m_1 m_2 \times N_1 N_2}$ .

## II. SYSTEM AND CHANNEL MODEL

The system consists of a BS equipped with  $N_{\text{tx}}$  antennas and  $J$  MTs. Each MT  $j \in \mathcal{J} = \{1, 2, \dots, J\}$  is equipped with  $N_{\text{rx}}$  antennas. We assume a block-fading model, cf., e.g., [30], where the DL signal for block  $t$  received at each MT  $j \in \mathcal{J}$  is

$$\mathbf{Y}_{j,t} = \mathbf{H}_{j,t} \mathbf{P}_t^T + \mathbf{N}_{j,t} \quad (1)$$

where  $t = 0, \dots, T$ , with the MIMO channel  $\mathbf{H}_{j,t} \in \mathbb{C}^{N_{\text{rx}} \times N_{\text{tx}}}$ , the pilot matrix  $\mathbf{P}_t \in \mathbb{C}^{n_p \times N_{\text{tx}}}$ , and the additive white Gaussian

noise (AWGN)  $\mathbf{N}_{j,t} = [\mathbf{n}'_{j,t,1}, \dots, \mathbf{n}'_{j,t,n_p}] \in \mathbb{C}^{N_{\text{rx}} \times n_p}$  with  $\mathbf{n}'_{j,t,p} \sim \mathcal{N}_{\mathbb{C}}(\mathbf{0}, \sigma_n^2 \mathbf{I}_{N_{\text{rx}}})$  for  $p \in \{1, 2, \dots, n_p\}$ , and  $n_p$  is the number of pilots. We consider systems with reduced pilot overhead, i.e.,  $n_p < N_{\text{tx}}$ . For the subsequent analysis, it is advantageous to vectorize (1):

$$\mathbf{y}_{j,t} = (\mathbf{P}_t \otimes \mathbf{I}_{N_{\text{rx}}}) \mathbf{h}_{j,t} + \mathbf{n}_{j,t} \quad (2)$$

where  $\mathbf{h}_{j,t} = \text{vec}(\mathbf{H}_{j,t})$ ,  $\mathbf{y}_{j,t} = \text{vec}(\mathbf{Y}_{j,t})$ ,  $\mathbf{n}_{j,t} = \text{vec}(\mathbf{N}_{j,t})$ , and  $\mathbf{n}_{j,t} \sim \mathcal{N}_{\mathbb{C}}(\mathbf{0}, \boldsymbol{\Sigma})$  with  $\boldsymbol{\Sigma} = \sigma_n^2 \mathbf{I}_{N_{\text{rx}} n_p}$ .

We adopt the 3rd Generation Partnership Project (3GPP) spatial channel model (see [30], [31]) where channels are modeled conditionally Gaussian, i.e.,  $\mathbf{h}_{j,t} | \boldsymbol{\delta}_j \sim \mathcal{N}_{\mathbb{C}}(\mathbf{0}, \mathbf{C}_{\boldsymbol{\delta}_j})$ . The covariance matrix of each MT  $\mathbf{C}_{\boldsymbol{\delta}_j}$  is assumed to remain constant over  $T+1$  blocks. The random vectors  $\boldsymbol{\delta}_j$  comprise the main angles of arrival/departure of the multi-path propagation cluster between the BS and MT  $j$ . The main angles of arrival/departure are drawn independently and are uniformly distributed over  $[-\frac{\pi}{2}, \frac{\pi}{2}]$ . At the BS as well as the MTs uniform linear arrays (ULAs) are deployed such that the transmit- and receive-side spatial channel covariance matrices are given by

$$\mathbf{C}_{\boldsymbol{\delta}_j}^{\{\text{rx}, \text{tx}\}} = \int_{-\pi}^{\pi} g^{\{\text{rx}, \text{tx}\}}(\theta; \boldsymbol{\delta}_j) \mathbf{a}^{\{\text{rx}, \text{tx}\}}(\theta) \mathbf{a}^{\{\text{rx}, \text{tx}\}, \text{H}}(\theta) d\theta, \quad (3)$$

where  $\mathbf{a}^{\{\text{rx}, \text{tx}\}}(\theta) = [1, e^{j\pi \sin(\theta)}, \dots, e^{j\pi(N_{\{\text{rx}, \text{tx}\}}-1)\sin(\theta)}]^T$  is the array steering vector for an angle of arrival/departure  $\theta$  and  $g^{\{\text{rx}, \text{tx}\}}$  is a Laplacian power density whose standard deviation describes the angular spread  $\sigma_{\text{AS}}^{\{\text{rx}, \text{tx}\}}$  of the propagation cluster at the BS ( $\sigma_{\text{AS}}^{\text{tx}} = 2^\circ$ ) and MT  $j$  ( $\sigma_{\text{AS}}^{\text{rx}} = 35^\circ$ ) side [31]. The overall channel covariance matrix per MT  $j$  is constructed as  $\mathbf{C}_{\boldsymbol{\delta}_j} = \mathbf{C}_{\boldsymbol{\delta}_j}^{\text{tx}} \otimes \mathbf{C}_{\boldsymbol{\delta}_j}^{\text{rx}}$  due to the assumption of independent scattering in the vicinity of transmitter and receiver, see, e.g., [32]. In the case of MTs equipped with a single antenna,  $\mathbf{C}_{\boldsymbol{\delta}_j}$  degenerates to the transmit-side covariance matrix  $\mathbf{C}_{\boldsymbol{\delta}_j}^{\text{tx}}$ . Due to the low angular spread at the BS side, the covariance matrices exhibit a low numerical rank. The channel model described above was similarly employed in [9], [10], where  $\boldsymbol{\delta}_j$  was assumed to be given for all  $j \in \mathcal{J}$ .

With

$$\mathcal{H} = \{\mathbf{h}^{(m)}\}_{m=1}^M, \quad (4)$$

we denote the training data set consisting of  $M$  channel samples, following [25], [33]. For every channel sample  $\mathbf{h}^{(m)}$ , we first generate random angles, collected in  $\boldsymbol{\delta}^{(m)}$ , and then draw the sample as  $\mathbf{h}^{(m)} \sim \mathcal{N}_{\mathbb{C}}(\mathbf{0}, \mathbf{C}_{\boldsymbol{\delta}^{(m)}})$ . The resulting data set represents a wireless communication environment with unknown PDF  $f_{\mathbf{h}}$ . Additionally, the channel of any MT located anywhere within the BS's coverage area can be interpreted as a realization of a random variable with this PDF  $f_{\mathbf{h}}$ .

Alternatively, environment-specific training data can be acquired, for instance, from a measurement campaign [34], [35] or by using a ray-tracing tool [36]. The analysis of these different training data sources is out of the scope of this work.

### III. POINT-TO-POINT MIMO SYSTEM

#### A. Pilot Optimization with Perfect Statistical Knowledge

In the case of a point-to-point MIMO system, we drop the index  $j$  in (2) for notational convenience, yielding

$$\mathbf{y}_t = (\mathbf{P}_t \otimes \mathbf{I}_{N_{\text{rx}}}) \mathbf{h}_t + \mathbf{n}_t. \quad (5)$$

Given genie knowledge of  $\boldsymbol{\delta}$ , which fully characterizes the channel statistically (cf. (3)), the observation  $\mathbf{y}_t$  is jointly Gaussian with the channel  $\mathbf{h}_t$ . Thus, we can compute a genie linear minimum mean square error (LMMSE) channel estimate via [30]

$$\begin{aligned} \hat{\mathbf{h}}_{t, \text{gLMMSE}} &= \mathbb{E}[\mathbf{h}_t | \mathbf{y}_t, \boldsymbol{\delta}] \\ &= \mathbf{C}_{\boldsymbol{\delta}} (\mathbf{P}_t \otimes \mathbf{I}_{N_{\text{rx}}})^{\text{H}} ((\mathbf{P}_t \otimes \mathbf{I}_{N_{\text{rx}}}) \mathbf{C}_{\boldsymbol{\delta}} (\mathbf{P}_t \otimes \mathbf{I}_{N_{\text{rx}}})^{\text{H}} + \boldsymbol{\Sigma})^{-1} \mathbf{y}_t. \end{aligned} \quad (6)$$

The goal of pilot optimization is to design the pilot matrix  $\mathbf{P}_t$  such that the MSE between  $\hat{\mathbf{h}}_{t, \text{gLMMSE}}$  and the actual channel  $\mathbf{h}_t$  is minimized [4], [7], [8]:

$$\mathbf{P}_t^* = \arg \min_{\mathbf{P}_t} \mathbb{E}[\|\hat{\mathbf{h}}_{t, \text{gLMMSE}} - \mathbf{h}_t\|^2] \quad (8)$$

where the pilot matrix  $\mathbf{P}_t$  typically satisfies either a total power constraint as in [7], [8] or an equal power per pilot vector constraint as in [4]. In this work, we consider the latter case. For a given  $\boldsymbol{\delta}$ , the optimal pilot matrix  $\mathbf{P}_t^*$  for every block is the same, i.e.,  $\mathbf{P}_t^* = \mathbf{P}_{\text{genie}}^*$  for all  $t = 0, \dots, T$ . In particular,  $\mathbf{P}_{\text{genie}}^*$  is a sub-unitary matrix [4]

$$\mathbf{P}_{\text{genie}}^* = \sqrt{\rho} \mathbf{U}_{\boldsymbol{\delta}}^{\text{H}}[:, n_p, :], \quad (9)$$

which is composed of the  $n_p$  dominant eigenvectors of the transmit-side covariance matrix  $\mathbf{C}_{\boldsymbol{\delta}}^{\text{tx}} = \mathbf{U}_{\boldsymbol{\delta}} \boldsymbol{\Lambda}_{\boldsymbol{\delta}} \mathbf{U}_{\boldsymbol{\delta}}^{\text{H}}$  corresponding to the  $n_p$  largest eigenvalues, where  $\rho$  denotes the transmit power per pilot vector.

Note that power loading across pilot vectors generally performs better but requires additional processing. Additionally, with a sub-unitary pilot design, our proposed scheme yields a codebook consisting of pilot matrices that do not depend on the SNR, resolving the burden of saving SNR level-specific pilot codebooks, see Section III-B4.

#### B. GMM-based Pilot Design and Downlink Channel Estimation

Any channel  $\mathbf{h}_t$  of a MT located anywhere within the BS's coverage area can be interpreted as a realization of a random variable with PDF  $f_{\mathbf{h}}$  for which, however, no analytical expression is available. To overcome this issue, we utilize a GMM to approximate the PDF  $f_{\mathbf{h}}$ , following [25], [27]. This learned model is then shared between the BS and the MT to establish common awareness of the channel characteristics. The GMM is afterward used to infer feedback information for pilot matrix design and for DL channel estimation at the MT in the online phase. Thereby, the feedback information of the MT of a preceding fading block  $t-1$  is leveraged at the BS to select the pilot matrix for the subsequent fading block  $t > 0$ .

1) *Modeling the Channel Characteristics at the BS – Offline:* The channel characteristics are captured offline using a GMM comprised of  $K = 2^B$  components,

$$f_{\mathbf{h}}^{(K)}(\mathbf{h}_t) = \sum_{k=1}^K \pi_k \mathcal{N}_{\mathbb{C}}(\mathbf{h}_t; \boldsymbol{\mu}_k, \mathbf{C}_k) \quad (10)$$

where each component of the GMM is defined by the mixing coefficient  $\pi_k$ , the mean  $\boldsymbol{\mu}_k$ , and the covariance matrix  $\mathbf{C}_k$ .

Motivated by the observation that the channel exhibits an unconditioned zero mean and similar to [33], we enforce the means of the GMM-components to zero, i.e.,  $\boldsymbol{\mu}_k = \mathbf{0}$  for all

$k \in \{1, \dots, K\}$ . In [37], a theoretical justification for this regularization is provided. This regularization also reduces the number of learnable parameters and, thus, prevents overfitting. Note that the parameters of the GMM, i.e.,  $\{\pi_k, \mathbf{C}_k\}_{k=1}^K$ , remain constant across all blocks. To obtain maximum likelihood estimates of the GMM parameters, we utilize the training data set  $\mathcal{H}$  [see (4)] and employ an expectation maximization (EM) algorithm, as described in [38, Subsec. 9.2.2], where we enforce the means to zero in every M-step of the EM algorithm.

For MIMO channels, we further impose a Kronecker factorization on the covariances of the GMM, i.e.,  $\mathbf{C}_k = \mathbf{C}_k^{\text{tx}} \otimes \mathbf{C}_k^{\text{rx}}$ . Thus, instead of fitting an unconstrained GMM with  $N \times N$ -dimensional covariances (where  $N = N_{\text{tx}}N_{\text{rx}}$ ), we fit separate GMMs for the transmit and receive sides. These transmit-side and receive-side GMMs possess  $N_{\text{tx}} \times N_{\text{tx}}$  and  $N_{\text{rx}} \times N_{\text{rx}}$ -dimensional covariances, respectively, with  $K_{\text{tx}}$  and  $K_{\text{rx}}$  components. Then, by computing the Kronecker products of the corresponding transmit- and receive-side covariance matrices, we obtain a GMM with  $K = K_{\text{tx}}K_{\text{rx}}$  components and  $N \times N$ -dimensional covariances. Imposing this constraint on the GMM covariances significantly decreases the duration of offline training, facilitates parallelization of the fitting process, and demands fewer training samples due to the reduced number of parameters to be learned, cf. [25], [27]. In addition, having access to a transmit-side covariance during pilot design in the online phase, as discussed in Section III-B4, is ensured.

Using a GMM, we can calculate the posterior probability that the channel  $\mathbf{h}_t$  stems from component  $k$  as [38, Sec. 9.2],

$$p(k | \mathbf{h}_t) = \frac{\pi_k \mathcal{N}_{\mathbb{C}}(\mathbf{h}_t; \mathbf{0}, \mathbf{C}_k)}{\sum_{i=1}^K \pi_i \mathcal{N}_{\mathbb{C}}(\mathbf{h}_t; \mathbf{0}, \mathbf{C}_i)}. \quad (11)$$

These posterior probabilities are commonly referred to as responsibilities.

2) *Sharing the Model with the MTs – Offline:* A MT requires access to the GMM parameters to infer the feedback information. Conceptually, this involves sharing the parameters  $\{\pi_k, \mathbf{C}_k\}_{k=1}^K$ , with the MTs upon entering the coverage area of the BS. This transfer is required only once since the GMM remains unchanged for a specific BS environment.

Incorporating model-based insights to restrict the GMM covariances, as discussed in Section III-B1, additionally significantly reduces the model transfer overhead. Due to specific antenna array geometries, the GMM covariances can be further constrained to a Toeplitz or block-Toeplitz matrix with Toeplitz blocks, in case of a ULA or uniform rectangular array (URA), respectively, cf. [37], [39], [40], with even fewer parameters. In [40], it is further discussed how GMMs with variable bit lengths can be obtained. However, these further structural constraints and the analysis with variable bit lengths are out of the scope of this work.

3) *Inferring the Feedback Information and Estimating the Channel at the MTs – Online:* In the online phase, the MT infers feedback information given the observation  $\mathbf{y}_t$  utilizing the GMM. The joint Gaussian nature of each GMM component [see (10)] combined with the AWGN, allows for simple computation of the GMM of the observations with the GMM

from (10) as

$$f_{\mathbf{y}}^{(K)}(\mathbf{y}_t) = \sum_{k=1}^K \pi_k \mathcal{N}_{\mathbb{C}}(\mathbf{y}_t; \mathbf{0}, (\mathbf{P}_t \otimes \mathbf{I}_{N_{\text{rx}}}) \mathbf{C}_k (\mathbf{P}_t \otimes \mathbf{I}_{N_{\text{rx}}})^{\text{H}} + \boldsymbol{\Sigma}). \quad (12)$$

Thus, the MT can compute the responsibilities based on the observations  $\mathbf{y}_t$  as

$$p(k | \mathbf{y}_t) = \frac{\pi_k \mathcal{N}_{\mathbb{C}}(\mathbf{y}_t; \mathbf{0}, (\mathbf{P}_t \otimes \mathbf{I}_{N_{\text{rx}}}) \mathbf{C}_k (\mathbf{P}_t \otimes \mathbf{I}_{N_{\text{rx}}})^{\text{H}} + \boldsymbol{\Sigma})}{\sum_{i=1}^K \pi_i \mathcal{N}_{\mathbb{C}}(\mathbf{y}_t; \mathbf{0}, (\mathbf{P}_t \otimes \mathbf{I}_{N_{\text{rx}}}) \mathbf{C}_i (\mathbf{P}_t \otimes \mathbf{I}_{N_{\text{rx}}})^{\text{H}} + \boldsymbol{\Sigma})}. \quad (13)$$

The feedback information  $k_t^*$  is then determined through a maximum a posteriori (MAP) estimation (cf. [27]) as

$$k_t^* = \arg \max_k p(k | \mathbf{y}_t) \quad (14)$$

where the index of the component with the highest responsibility for the observation  $\mathbf{y}_t$  serves as the corresponding feedback information. Hence, the feedback information is simply the index of the GMM component that best explains the underlying channel  $\mathbf{h}_t$  for a given observation  $\mathbf{y}_t$ . Subsequently, the responsibilities are utilized to obtain a channel estimate via the GMM by calculating a convex combination of per-component LMMSE estimates, as discussed in [25], [27]. In particular, the MT estimates the channel by computing

$$\hat{\mathbf{h}}_{t,\text{GMM}}(\mathbf{y}_t) = \sum_{k=1}^K p(k | \mathbf{y}_t) \hat{\mathbf{h}}_{t,\text{LMMSE},k}(\mathbf{y}_t), \quad (15)$$

using the responsibilities  $p(k | \mathbf{y}_t)$  from (13) and

$$\begin{aligned} \hat{\mathbf{h}}_{t,\text{LMMSE},k}(\mathbf{y}_t) \\ = \mathbf{C}_k (\mathbf{P}_t \otimes \mathbf{I}_{N_{\text{rx}}})^{\text{H}} ((\mathbf{P}_t \otimes \mathbf{I}_{N_{\text{rx}}}) \mathbf{C}_k (\mathbf{P}_t \otimes \mathbf{I}_{N_{\text{rx}}})^{\text{H}} + \boldsymbol{\Sigma})^{-1} \mathbf{y}_t. \end{aligned} \quad (16)$$

Note that parallelization concerning the number of components  $K$  is possible during the feedback inference and the application of the LMMSE filters. Although the GMM estimator is a natural choice due to the usage of the responsibilities, which are anyway computed to determine the feedback information, in principle, any other channel estimator can be used.

4) *Designing the Pilots at the BS – Online:* Consider the eigenvalue decomposition of each of the GMM's transmit-side covariances, i.e.,  $\mathbf{C}_k^{\text{tx}} = \mathbf{U}_k \boldsymbol{\Lambda}_k \mathbf{U}_k^{\text{H}}$ . For  $t > 0$ , given the feedback information  $k_{t-1}^*$  of the MT from the preceding block  $t-1$ , we propose employing the pilot matrix  $\mathbf{P}_t$  at the BS for the subsequent block  $t$  as (cf. (9))

$$\mathbf{P}_t = \sqrt{\rho} \mathbf{U}_{k_{t-1}^*}^{\text{H}}[:, n_{\text{p}}, :], \quad (17)$$

i.e., the  $n_{\text{p}}$  dominant eigenvectors of the  $k_{t-1}^*$ -th transmit-side covariance matrix  $\mathbf{C}_{k_{t-1}^*}^{\text{tx}}$  are selected as the pilot matrix. Since the GMM-covariances remain fixed, we can store a set of pilot matrices  $\mathcal{P} = \{\mathbf{U}_k^{\text{H}}[:, n_{\text{p}}, :]\}_{k=1}^K$ , and the online pilot design utilizing the proposed GMM-based scheme simplifies to a simple selection task based on the feedback information  $k_{t-1}^*$  from the previous block. For the initial block  $t=0$ , we employ a discrete Fourier transform (DFT)-based pilot matrix.

## IV. MULTI-USER MIMO SYSTEM

### A. Pilot Optimization with Perfect Statistical Knowledge

Two well-established possibilities for designing pilot sequences for multi-user setups with single-antenna MTs were

introduced in [9], [10]. The method proposed in [9] utilizes the close relationship between the mutual information and the MSE [12] to design pilot sequences that maximize the sum CMI expression subject to a transmit power budget. Accordingly, the sum mutual information between each MT's channel  $\mathbf{h}_{j,t}$  and the observations  $\mathbf{y}_{j,t}$  conditioned on the transmitted pilot matrix  $\mathbf{P}_t$  is considered. We refer to [9] for systems where the MTs are equipped with a single antenna. In the following, we extend the framework from [9] to systems where the MTs are equipped with multiple antennas, i.e., to MU-MIMO systems.

The sum CMI maximization problem for MU-MIMO systems for a given number of pilots  $n_p$  and transmit power budget  $\rho$  is expressed as

$$\begin{aligned} \max_{\mathbf{P}_t} \quad & \sum_{j=1}^J \log \det \left( \mathbf{I} + \frac{1}{\sigma_n^2} (\mathbf{P}_t \otimes \mathbf{I}_{N_{\text{rx}}}) \mathbf{C}_{\delta_j} (\mathbf{P}_t \otimes \mathbf{I}_{N_{\text{rx}}})^{\text{H}} \right) \\ \text{s.t.} \quad & \text{tr}(\mathbf{P}_t \mathbf{P}_t^{\text{H}}) \leq \rho n_p. \end{aligned} \quad (18)$$

For given  $\{\delta_j\}_{j=1}^J$ , the optimal pilot matrix  $\mathbf{P}_t^*$  for every block is the same, i.e.,  $\mathbf{P}_t^* = \mathbf{P}_{\text{genie}}$  for all  $t = 0, \dots, T$ , and we establish the following theorem.

**Theorem 1.** *The pilot matrix  $\mathbf{P}_t^*$  that maximizes the sum CMI in a MU-MIMO system provided in (18) satisfies the condition*

$$\sum_{j=1}^J \sum_{i=1}^I \frac{1}{\sigma_n^2} \mathbf{V}_j \mathbf{D}_{\beta_{j,i}} \mathbf{V}_j^{\text{H}} \mathbf{P}_t^* \mathbf{C}_{\delta_j}^{\text{tx}} \text{tr}(\mathbf{D}_{\gamma_{j,i}} \mathbf{T}_j) = \lambda \mathbf{P}_t^*, \quad (19)$$

with the singular value decompositions (SVDs) for all  $j \in \mathcal{J}$ ,

$$\mathbf{P}_t^* \mathbf{C}_{\delta_j}^{\text{tx}} \mathbf{P}_t^{*\text{H}} = \mathbf{V}_j \mathbf{S}_j \mathbf{V}_j^{\text{H}}, \quad (20)$$

$$\mathbf{C}_{\delta_j}^{\text{rx}} = \mathbf{W}_j \mathbf{T}_j \mathbf{W}_j^{\text{H}}. \quad (21)$$

Further, let  $\sum_{i=1}^I \alpha_{j,i} \gamma_{j,i} \beta_{j,i}^{\text{T}}$  with  $I = \min(n_p, N_{\text{rx}})$ , be the SVD of the matrix  $\text{unvec}_{N_{\text{rx}}, n_p} \left( \text{diag} \left( (\mathbf{I} + \frac{1}{\sigma_n^2} \mathbf{S}_j \otimes \mathbf{T}_j)^{-1} \right) \right)$ . Then, the diagonal matrices  $\mathbf{D}_{\beta_{j,i}} \in \mathbb{R}^{n_p \times n_p}$  and  $\mathbf{D}_{\gamma_{j,i}} \in \mathbb{R}^{N_{\text{rx}} \times N_{\text{rx}}}$  for all  $j \in \mathcal{J}$ , in (19), are defined as

$$\mathbf{D}_{\beta_{j,i}} = \alpha_{j,i} \text{diag}(\beta_{j,i}), \quad (22)$$

$$\mathbf{D}_{\gamma_{j,i}} = \text{diag}(\gamma_{j,i}), \quad (23)$$

and  $\lambda \geq 0$  is a constant chosen to satisfy the power constraint.

*Proof.* See Appendix A.  $\square$

In the following corollary, we consider the special case with  $n_p \leq N_{\text{rx}}$ , which allows for a simplification.

**Corollary 1.1.** *The pilot matrix  $\mathbf{P}_t^*$  that maximizes the sum CMI in a MU-MIMO system provided in (18) with  $n_p \leq N_{\text{rx}}$  satisfies the condition*

$$\sum_{j=1}^J \sum_{i=1}^{n_p} \frac{1}{\sigma_n^2} \mathbf{v}_{j,i} \mathbf{v}_{j,i}^{\text{H}} \mathbf{P}_t^* \mathbf{C}_{\delta_j}^{\text{tx}} \text{tr}(\mathbf{D}_{j,i} \mathbf{T}_j) = \lambda \mathbf{P}_t^*, \quad (24)$$

utilizing the SVDs for all  $j \in \mathcal{J}$  from (20) and (21), where  $\mathbf{v}_{j,i}$  denotes the  $i$ -th column of  $\mathbf{V}_j$ , and

$$\begin{aligned} & (\mathbf{I} + \frac{1}{\sigma_n^2} \mathbf{S}_j \otimes \mathbf{T}_j)^{-1} \\ &= \text{diag}([d_{j,1}, \dots, d_{j,n_p N_{\text{rx}}}]^{\text{T}}) = \sum_{i=1}^{n_p} \text{diag}(\mathbf{e}_i) \otimes \mathbf{D}_{j,i}, \end{aligned} \quad (25)$$

---

**Algorithm 1** Iterative Pilot Matrix Design for MU-MIMO Systems

---

- 1: For  $\ell = 0$ , initialize pilot matrix  $\mathbf{P}_t^{(0)}$ , and set maximum number of iterations  $L_{\text{max}}$ . Compute SVDs for all  $j \in \mathcal{J}$ ,  $\mathbf{C}_{\delta_j}^{\text{rx}} = \mathbf{W}_j \mathbf{T}_j \mathbf{W}_j^{\text{H}}$ . Set  $\varepsilon$ . Set  $\ell = 1$ .
  - 2: **repeat**
  - 3:   Compute SVDs for all  $j \in \mathcal{J}$ ,  
 $\mathbf{P}_t^{(\ell-1)} \mathbf{C}_{\delta_j}^{\text{tx}} \mathbf{P}_t^{(\ell-1)\text{H}} = \mathbf{V}_j^{(\ell-1)} \mathbf{S}_j^{(\ell-1)} \mathbf{V}_j^{(\ell-1)\text{H}}$
  - 4:   Compute real-valued SVDs for all  $j \in \mathcal{J}$ ,  $I = \min(n_p, N_{\text{rx}})$ ,  
 $\sum_{i=1}^I \alpha_{j,i}^{(\ell-1)} \gamma_{j,i}^{(\ell-1)} \beta_{j,i}^{(\ell-1)\text{T}}$   
 $= \text{unvec}_{N_{\text{rx}}, n_p} \left( \text{diag} \left( (\mathbf{I} + \frac{1}{\sigma_n^2} \mathbf{S}_j^{(\ell-1)} \otimes \mathbf{T}_j)^{-1} \right) \right)$
  - 5:   Set for all  $j$  and  $i$ ,  
 $\mathbf{D}_{\beta_{j,i}}^{(\ell-1)} = \alpha_{j,i}^{(\ell-1)} \text{diag}(\beta_{j,i}^{(\ell-1)})$   
 $\mathbf{D}_{\gamma_{j,i}}^{(\ell-1)} = \text{diag}(\gamma_{j,i}^{(\ell-1)})$
  - 6:   Calculate intermediate pilot matrix  $\tilde{\mathbf{P}}_t^{(\ell)}$   
 $= \sum_{j=1}^J \sum_{i=1}^I \frac{\text{tr}(\mathbf{D}_{\gamma_{j,i}}^{(\ell-1)} \mathbf{T}_j)}{\sigma_n^2} \mathbf{V}_j^{(\ell-1)} \mathbf{D}_{\beta_{j,i}}^{(\ell-1)} \mathbf{V}_j^{(\ell-1)\text{H}} \mathbf{P}_t^{(\ell-1)} \mathbf{C}_{\delta_j}^{\text{tx}}$
  - 7:   Apply Normalization to fulfill power constraint,  
 $\mathbf{P}_t^{(\ell)} = \sqrt{\frac{\rho n_p}{\text{tr}(\tilde{\mathbf{P}}_t^{(\ell)} \tilde{\mathbf{P}}_t^{(\ell)\text{H}})}} \tilde{\mathbf{P}}_t^{(\ell)}$
  - 8:    $\ell \leftarrow \ell + 1$
  - 9: **until** Spectral norm  $\|\mathbf{P}_t^{(\ell)} - \mathbf{P}_t^{(\ell-1)}\|_2 < \varepsilon$  or  $\ell \geq L_{\text{max}}$ .
- 

with the  $n_p$ -dimensional vectors  $\mathbf{e}_i$ , and  $\mathbf{D}_{j,i} = \text{diag}([d_{j,(i-1)N_{\text{rx}}+1}, \dots, d_{j,iN_{\text{rx}}}]^{\text{T}})$ , cf. (38), where  $\lambda \geq 0$  is a constant chosen to satisfy the power constraint.

Note that in (25) we used that any diagonal matrix  $\mathbf{D} \in \mathbb{R}^{n_p N_{\text{rx}} \times n_p N_{\text{rx}}}$  with  $n_p \leq N_{\text{rx}}$  can be decomposed as  $\mathbf{D} = \text{diag}([d_1, \dots, d_{n_p N_{\text{rx}}}]^{\text{T}}) = \sum_{i=1}^{n_p} \text{diag}(\mathbf{e}_i) \otimes \mathbf{D}_i$ , with the  $n_p$ -dimensional vectors  $\mathbf{e}_i$ , and the  $(N_{\text{rx}} \times N_{\text{rx}})$ -dimensional diagonal matrices  $\mathbf{D}_i = \text{diag}([d_{(i-1)N_{\text{rx}}+1}, \dots, d_{iN_{\text{rx}}}]^{\text{T}})$ .

In general, the optimization problem in (18) is a non-convex problem (see the discussion at the end of this subsection). Thus, similar to the algorithm for MTs with single antennas [9], we outline an iterative algorithm that aims to find the optimal pilot matrix based on the first-order Karush-Kuhn-Tucker (KKT) condition for MU-MIMO systems in Algorithm 1. Throughout this work, we have  $\varepsilon = 10^{-3}$ . As initialization, we apply either a random pilot matrix or a random selection of columns of an (oversampled) DFT matrix for  $\mathbf{P}_t^{(0)}$ . We discuss the effect of the initialization as well as the specific selection of the maximum number of iterations  $L_{\text{max}}$  on the algorithm's performance in Section VIII-B.

To reduce the computational overhead of optimizing (18), we establish a lower bound on the sum CMI expression serving as an approximate objective. We further present conditions on when the lower bound exhibits the largest gap to the sum CMI and when the lower bound is equal to the sum CMI. Accordingly, it is possible to maximize the established lower bound expression instead of the sum CMI.

**Theorem 2.** *The sum CMI expression of a MU-MIMO system provided as the utility function in (18) can be lower bounded by*

$$\sum_{j=1}^J \log \det \left( \mathbf{I} + \frac{1}{\sigma_n^2} (\mathbf{P}_t \text{tr}(\mathbf{C}_{\delta_j}^{\text{rx}}) \mathbf{C}_{\delta_j}^{\text{tx}} \mathbf{P}_t^{\text{H}}) \right). \quad (26)$$

*Proof.* See Appendix B.  $\square$

**Proposition 2.1.** *The lower bound expression from (26) is equal to the sum CMI in a MU-MIMO system provided in (18) for the same but arbitrary  $\mathbf{P}_t$  if and only if for all  $j \in \mathcal{J}$*

$$\text{rk}(\mathbf{C}_{\delta_j}^{\text{rx}}) = 1. \quad (27)$$

*Proof.* See Appendix C.  $\square$

**Proposition 2.2.** *The lower bound expression from (26) attains the largest gap to the sum CMI in a MU-MIMO system provided in (18) for the same but arbitrary  $\mathbf{P}_t$ , with fixed traces  $\tau_j = \text{tr}(\mathbf{C}_{\delta_j}^{\text{rx}})$ , if and only if for all  $j \in \mathcal{J}$*

$$\frac{1}{\tau_j} \mathbf{C}_{\delta_j}^{\text{rx}} = \frac{1}{N_{\text{rx}}} \mathbf{I}. \quad (28)$$

*Proof.* See Appendix D.  $\square$

**Corollary 2.1.** *In conjunction with [9, Th. 1], the optimal pilot matrix  $\mathbf{P}_t^*$  which maximizes the lower bound expression in (26) satisfies the condition*

$$\sum_{j=1}^J \frac{1}{\sigma_n^2} \left( \mathbf{I} + \frac{1}{\sigma_n^2} \mathbf{P}_t^* \text{tr}(\mathbf{C}_{\delta_j}^{\text{rx}}) \mathbf{C}_{\delta_j}^{\text{tx}} \mathbf{P}_t^{*,\text{H}} \right)^{-1} \mathbf{P}_t^* \text{tr}(\mathbf{C}_{\delta_j}^{\text{rx}}) \mathbf{C}_{\delta_j}^{\text{tx}} = \lambda \mathbf{P}_t^*. \quad (29)$$

Due to Proposition 2.1, there are cases where the lower bound provided in Theorem 2 equals to the MU-MISO sum CMI expression (with additional scaling by  $\text{tr}(\mathbf{C}_{\delta_j}^{\text{rx}})$  for all  $j \in \mathcal{J}$ ) in [9] and consequently [9, Remark 1] can be utilized to show that the MU-MIMO sum CMI maximization problem in (18) is not a convex problem.

The sum CMI expression in (18) can be replaced by the lower bound expression from (26). Then, the resulting objective resembles the MU-MISO sum CMI maximization as in [9] with the additional scaling of the transmit side covariance matrix  $\mathbf{C}_{\delta_j}^{\text{tx}}$  with  $\text{tr}(\mathbf{C}_{\delta_j}^{\text{rx}})$  for all  $j \in \mathcal{J}$ . The main advantage of the lower bound maximization is a reduced computational complexity (see Section VI) compared to solving the original problem in (18), since as a consequence to Theorem 2 and Corollary 2.1, the MU-MISO optimizer from [9] can be used for pilot design.

### B. Conventional Multi-User Pilot Matrix Signaling

In general, each of the MTs is unaware of the statistics of the other MTs. Thus, after designing the pilot matrix at the BS following either the iterative Algorithm 1 outlined in Section IV-A utilizing Theorem 1 or using the optimizer from [9] due to Theorem 2, the pilot matrix needs to be transferred from the BS to the MTs. Transferring the complete pilot matrix to the MTs might result in a significant signaling overhead that contradicts the initial goal of training overhead reduction [10], [41]. A conventional state-of-the-art solution that avoids transferring the complete pilot matrix was introduced in [10]. There, a codebook  $\mathcal{C}_{\text{RMP}}$ , with  $|\mathcal{C}_{\text{RMP}}| = 2^{B_{\text{RMP}}}$ , known to the BS and all MTs is used to quantize the  $n_p$  pilot vectors of the pilot matrix. Subsequently, the selected codebook elements indices are broadcasted to all MTs using a limited feedforward link. The method proposed in [10] avoids a brute force search of the codebook elements and instead relies on the so-called range matching pursuit (RMP) algorithm [10, Algorithm 2]. Thereby, the span of the resulting pilot matrix, which can be encoded

by in total  $n_p B_{\text{RMP}}$  bits, provides the best approximation of the span of the originally designed pilot matrix. As suggested in [10], [41], the  $N_{\text{tx}}$ -dimensional columns of an oversampled DFT matrix are selected as the elements of the codebook  $\mathcal{C}_{\text{RMP}}$ .

### C. GMM-based Multi-User Pilot Matrix Design and Signaling

In the multi-user case, we can exploit the same GMM as in the single-user case and, thus, require no additional training or adjustment. We propose that each MT  $j$  determines its feedback information via a MAP estimation, similar to the single-user case, as

$$k_{j,t}^* = \arg \max_k p(k | \mathbf{y}_{j,t}). \quad (30)$$

For  $t > 0$ , given the feedback information  $\{k_{j,t-1}^*\}_{j=1}^J$  of all MTs from the preceding block  $t-1$ , we propose designing the pilot matrix  $\mathbf{P}_t$  at the BS for the subsequent block  $t$  by utilizing the respective GMM-component's covariance information (cf. Section III-B1)

$$\{\mathbf{C}_{k_{j,t-1}^*} = \mathbf{C}_{k_{j,t-1}^*}^{\text{tx}} \otimes \mathbf{C}_{k_{j,t-1}^*}^{\text{rx}}\}_{j=1}^J \quad (31)$$

associated with  $\{k_{j,t-1}^*\}_{j=1}^J$ . At the BS, the covariance information obtained with the help of the GMM can then be leveraged to design the pilot matrix  $\mathbf{P}_t$  by either applying the iterative algorithm (Algorithm 1) outlined in Section IV-A following Theorem 1 or using the iterative algorithm from [9] following Corollary 2.1. For the initial block  $t=0$ , we employ a random selection of columns of an (oversampled) DFT matrix as the pilot matrix. Also, in this case, the MTs are in general unaware of the statistics of the other MTs, or in this particular case, the covariance information associated with the GMM components. In contrast to the conventional feedforward signaling (see Section IV-B), we propose to broadcast the feedback information  $\{k_{j,t-1}^*\}_{j=1}^J$  of all MTs using a feedforward link to all MTs, i.e., the BS first collects the feedback indices of all MTs and subsequently feedforwards them to all MTs. Accordingly, the feedforward information is encoded by  $JB$  bits. This approach requires each MT to design the pilot matrix locally in order to achieve the common pilot matrix knowledge required for the next fading block. Thereby, the computational effort at the MTs can be kept low by either utilizing the lower bound optimization approach or restricting the maximum number of iterations  $L_{\text{max}}$  of the iterative algorithm outlined in Section IV-A. Furthermore, the initialization of the pilot matrix of the iterative algorithm needs to be based on the same initial pilot matrix. We use the DFT matrix, which is used in the zeroth block or a random pilot matrix as the initial pilot matrix. The effect of the specific initialization, the selection of  $L_{\text{max}}$ , and the choice of the optimization approach allows for a complexity-to-performance trade-off and are discussed in Section VI and Section VIII-B.

## V. DISCUSSION ON THE VERSATILITY OF THE PROPOSED PILOT MATRIX DESIGN SCHEME

After fitting the GMM at the BS offline, the model from (10) is offloaded, i.e., the model parameters are transferred to every MT within the coverage area of the BS. In the online phase, at the MTs, the GMM of the observations [see (12)]

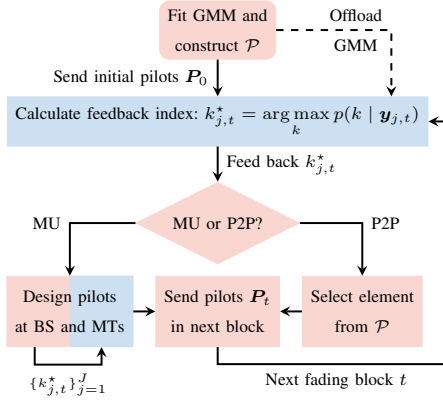


Fig. 1: Flowchart of the versatile pilot matrix design scheme. Red (blue) colored nodes are processed at the BS (MTs) and solid (dashed) arrows indicate online (offline) processing.

can be constructed depending on the pilots and SNR level and does not require re-training. By utilizing the GMM of the observations, each MT can infer its feedback information  $k_{j,t}^*$  by evaluating (30), which is subsequently fed back to the BS. The BS can then decide to either serve one MT in the point-to-point mode or all MTs simultaneously in the multi-user mode. In the single-user mode, the BS simply selects the pilot matrix associated with the MT's feedback information of the preceding block  $k_{j,t-1}^*$  from the pilot codebook  $\mathcal{P}$ , see Section III-B4, and no further processing is required. In the multi-user mode, a feedforward link is required to broadcast the feedback information  $\{k_{j,t-1}^*\}_{j=1}^J$  of all MTs from the BS to all MTs. Then, the pilot matrix  $\mathbf{P}_t$  for the subsequent fading block can be obtained at the BS and MTs utilizing either the iterative algorithm (Algorithm 1) outlined in Section IV-A following Theorem 1 or using the iterative algorithm from [9] following Corollary 2.1. The flexibility regarding the transmission mode, together with the possibility to serve any desired number of MTs  $J$ , in combination with the straightforward adaption to any number of pilots  $n_p$  and SNR level, highlights the versatility of the proposed GMM-based pilot design scheme. The proposed versatile pilot design scheme is summarized as a flowchart in Fig. 1, where red (blue) colored nodes represent processing steps that are performed at the BS (MTs).

## VI. COMPLEXITY ANALYSIS

The online computational complexity of the proposed GMM-based scheme can be divided into three parts:

1) *Inference of the Feedback Information:* Matrix-vector multiplications dominate the computational complexity for inferring the feedback information at the MTs. This is because the computation of the responsibilities in (13) entails evaluating Gaussian densities, and the calculations involving determinants and inverses can be pre-computed for a specific SNR level due to the fixed GMM parameters. Thus, the inference of the feedback information using (30) in the online phase at each MT has a complexity of  $\mathcal{O}(KN_{\text{rx}}^2 n_p^2)$ , where parallelization concerning the number of components  $K$  is possible.

2) *Pilot Matrix Design:* The computational complexity of the online pilot matrix design depends on the transmission mode, i.e., single- or multi-user mode.

In the single-user mode, the computational complexity is  $\mathcal{O}(K)$ , as it only involves traversing the pre-computed set of

pilot matrices  $\mathcal{P}$ . Thus, in the online phase, our scheme avoids computing an eigenvalue decomposition, which is required for solving the optimization problem from (8).

The computational complexity in the multi-user mode depends on the applied optimization algorithm. In case of the iterative algorithm outlined in Section IV-A following Theorem 1, the computational complexity per iteration is  $\mathcal{O}(J(n_p N_{\text{tx}}^2 + n_p^2 N_{\text{tx}} \min(n_p, N_{\text{rx}})))$ . Alternatively, using the iterative algorithm from [9] following Corollary 2.1 exhibits a complexity of  $\mathcal{O}(J n_p N_{\text{tx}}^2)$  per iteration.

3) *Channel Estimation:* Processing the responsibilities to an estimated channel with the GMM via (15) exhibits a computational complexity of  $\mathcal{O}(KN_{\text{rx}}^2 N_{\text{tx}} n_p)$ , since also the LMMSE filters for a given SNR level can be pre-computed. Similar to the feedback inference, parallelization concerning the number of components  $K$  is possible when applying the LMMSE filters. As discussed before, in general, any other channel estimator can be used.

## VII. BASELINE ESTIMATORS AND PILOT SCHEMES

Since channel estimation is performed independently at each MT, we discuss the estimators from a single MT perspective and omit the index  $j$  for simplicity. In addition to the utopian genie LMMSE approach (6), where we assume perfect knowledge of  $\delta$  at the BS to design the optimal pilots and at the MT to apply the genie LMMSE estimator, we consider the following channel estimators and pilot matrices.

Firstly, we consider the LMMSE estimator  $\hat{h}_{\text{LMMSE}}$ , where the sample covariance matrix is formed using the set  $\mathcal{H}$  [see (4)], as discussed in, e.g., [25], [27].

Secondly, we consider a compressive sensing estimation method  $\hat{h}_{\text{OMP}}$  employing the orthogonal matching pursuit (OMP) algorithm, cf. [42], [43]. Since the sparsity order is unknown, but the algorithm's performance heavily depends on it, we use a genie-aided approach to obtain a bound on the algorithm's performance. Specifically, we use perfect channel knowledge to select the optimal sparsity order, cf. [25], [27].

Additionally, we compare to an end-to-end DNN approach for DL channel estimation with a jointly learned pilot matrix  $\mathbf{P}_{\text{DNN}}$ , similar to [13], [14]. To determine the hyperparameters of the DNN, we utilize random search [44], with the MSE serving as the loss function. The DNN architecture comprises  $D_{\text{CM}}$  convolutional modules, each consisting of a convolutional layer, batch normalization, and an activation function, where  $D_{\text{CM}}$  is randomly selected within [3, 9]. Each convolutional layer contains  $D_{\text{K}}$  kernels, where  $D_{\text{K}}$  is randomly selected within [32, 64]. The activation function in each convolutional module is the same and is randomly selected from {ReLU, sigmoid, PReLU, Leaky ReLU, tanh, swish}. Following a subsequent two-dimensional max-pooling, the features are flattened, and a fully connected layer is employed with an output dimension of  $2N_{\text{tx}}N_{\text{rx}}$  (concatenated real and imaginary parts of the estimated channel). We train a distinct DNN for each pilot configuration and SNR level, running 50 random searches per pilot configuration and SNR level and selecting the best-performing DNN for each setup.

Lastly, as further baseline pilot matrices, we utilize a DFT sub-matrix  $\mathbf{P}_{\text{DFT}}$  as the pilot matrix, see, e.g., [45], and

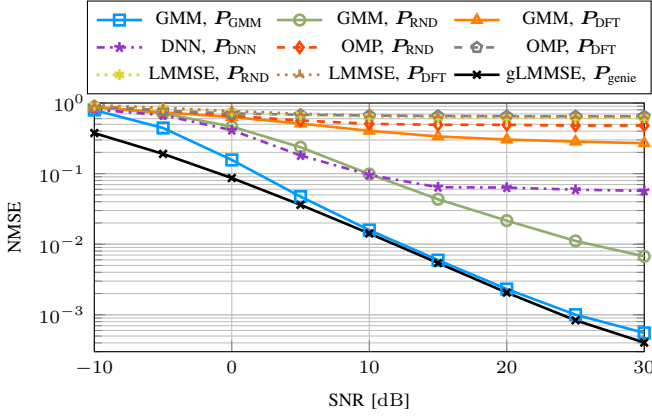


Fig. 2: The NMSE over the SNR for a MIMO system ( $N_{\text{tx}} = 16$ ,  $N_{\text{rx}} = 4$ ) with  $B = 7$  feedback bits and  $n_p = 4$  pilots.

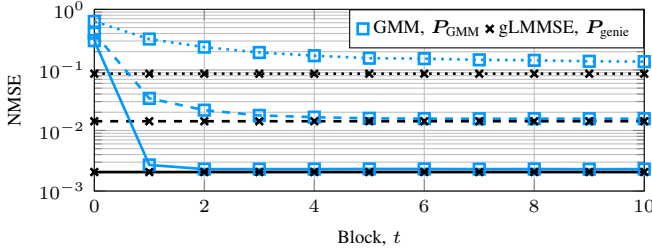


Fig. 3: The NMSE over the block index  $t$  for a MIMO system ( $N_{\text{tx}} = 16$ ,  $N_{\text{rx}} = 4$ ) with  $B = 7$  feedback bits,  $n_p = 4$  pilots, for different SNR levels (dotted: 0 dB, dashed: 10 dB, solid: 20 dB).

alternatively, we consider random pilot matrices denoted by  $\mathbf{P}_{\text{RND}}$ , see, e.g., [8].

## VIII. SIMULATION RESULTS

We use the set  $\mathcal{H}$  [see (4)] with  $M = 10^5$  samples for fitting the GMM and all other data-aided baselines. We use a different data set of  $M_{\text{eval}} = 10^4$  channel samples per block  $t$  for evaluation purposes, where we set  $T = 10$ . The data samples are normalized to satisfy  $\mathbb{E}[\|\mathbf{h}\|^2] = N = N_{\text{tx}}N_{\text{rx}}$ . Additionally, we fix  $\rho = 1$ , enabling the definition of the SNR as  $\frac{1}{\sigma_n^2}$ . We employ the normalized MSE (NMSE) as the performance measure. Specifically, for every block  $t$ , we compute a corresponding channel estimate  $\hat{\mathbf{h}}^{(m_{\text{eval}})}$  for each test channel in the set  $\{\mathbf{h}^{(m_{\text{eval}})}\}_{m_{\text{eval}}=1}^{M_{\text{eval}}}$ , and calculate  $\text{NMSE} = \frac{1}{NM_{\text{eval}}} \sum_{m_{\text{eval}}=1}^{M_{\text{eval}}} \|\mathbf{h}^{(m_{\text{eval}})} - \hat{\mathbf{h}}^{(m_{\text{eval}})}\|^2$ . If not mentioned otherwise, we consider the block with index  $t = 5$  in the subsequent simulations.

### A. Point-to-point MIMO

In Fig. 2, we simulate a system with  $N_{\text{tx}} = 16$  BS antennas,  $N_{\text{rx}} = 4$  MT antennas, and  $n_p = 4$  pilots. Since we have a MIMO setup, we fit a Kronecker-structured GMM with in total  $K = 2^7 = 128$  components ( $B = 7$  feedback bits), where  $K_{\text{tx}} = 32$  and  $K_{\text{rx}} = 4$ . The proposed GMM-based pilot design scheme (see Section III-B) denoted by “GMM,  $\mathbf{P}_{\text{GMM}}$ ” outperforms all baselines “{GMM, OMP, LMMSE}, { $\mathbf{P}_{\text{DFT}}$ ,  $\mathbf{P}_{\text{RND}}$ }” by a large margin, where the GMM estimator, the OMP-based estimator, or the LMMSE estimator, are used in combination with either DFT-based pilot matrices or random pilot matrices. The proposed scheme also outperforms the DNN based approach denoted by “DNN,  $\mathbf{P}_{\text{DNN}}$ ,” which jointly learns

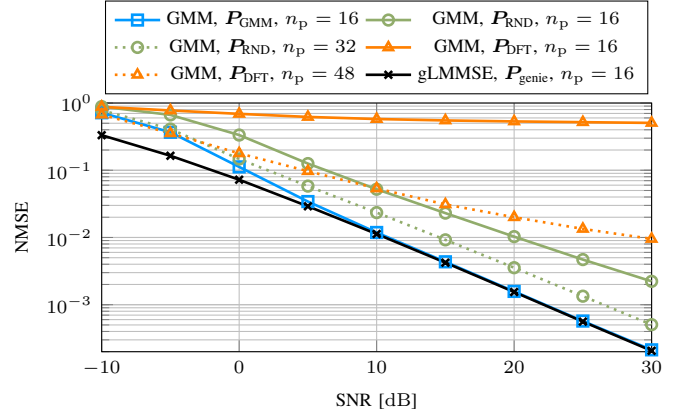


Fig. 4: The NMSE over the SNR for a MISO system ( $N_{\text{tx}} = 64$ ,  $N_{\text{rx}} = 1$ ) with  $B = 6$  feedback bits and  $n_p \in \{16, 32, 48\}$  pilots.

the estimator and a global pilot matrix for the whole scenario; thus, it cannot provide an MT adaptive pilot matrix. This highlights the advantage of the proposed model-based technique over the end-to-end learning technique, which is even trained for each SNR level and pilot configuration. Furthermore, we can observe that the GMM-based pilot design scheme performs only slightly worse than the baseline with perfect statistical information at the BS and MT [see (6) and (9)], denoted by “gLMMSE,  $\mathbf{P}_{\text{genie}}$ ,” being a utopian estimation approach. We can observe a larger gap in the low SNR regime, where the feedback information obtained through the responsibilities of a given observation [see (14)] is less accurate due to high noise.

In Fig. 3, we analyze the performance of the proposed GMM-based pilot design scheme over the block index  $t$  for the same setup as before at three different SNR levels, i.e.,  $\text{SNR} \in \{0 \text{ dB}, 10 \text{ dB}, 20 \text{ dB}\}$ . As discussed in Section III-B4, at  $t = 0$ , we utilize DFT-based pilots. At  $t = 1$ , we can already see a significant gain in performance of the proposed GMM-based pilot design scheme due to the feedback of the index. The results further reveal that with an increasing SNR, fewer blocks are required to achieve a performance close to the utopian baseline “gLMMSE,  $\mathbf{P}_{\text{genie}}$ ” which requires perfect statistical knowledge at the BS and the MT.

In the remainder, we consider a MISO system with  $N_{\text{tx}} = 64$  BS antennas and  $N_{\text{rx}} = 1$  antenna at the MT. In Fig. 4 we utilize a GMM with  $K = 2^6 = 64$  components ( $B = 6$  feedback bits) and consider setups with  $n_p \in \{16, 32, 48\}$  pilots. In this case, the proposed scheme “GMM,  $\mathbf{P}_{\text{GMM}}$ ,  $n_p = 16$ ,” performs only slightly worse than the genie-aided approach “gLMMSE,  $\mathbf{P}_{\text{genie}}$ .” Moreover, the GMM-based pilot design scheme outperforms the baselines “GMM, { $\mathbf{P}_{\text{DFT}}$ ,  $\mathbf{P}_{\text{RND}}$ },  $n_p \in \{16, 32, 48\}$ .” In particular, the proposed scheme with only  $n_p = 16$  pilots outperforms random pilot matrices with twice as much pilots ( $n_p = 32$ ) or in case of DFT-based pilots even thrice as much pilots ( $n_p = 48$ ).

Lastly, in Fig. 5, we analyze the effect of varying the number of GMM-components  $K$ , on the scheme’s performance, where we set  $n_p = 16$  and consider three different SNR levels, i.e.,  $\text{SNR} \in \{0 \text{ dB}, 10 \text{ dB}, 20 \text{ dB}\}$ . We observe that the estimation error decreases as the number of components  $K$  increases. Moreover, as the SNR increases, the gap to the genie-aided approach “gLMMSE,  $\mathbf{P}_{\text{genie}}$ ” narrows. Above  $K = 32$



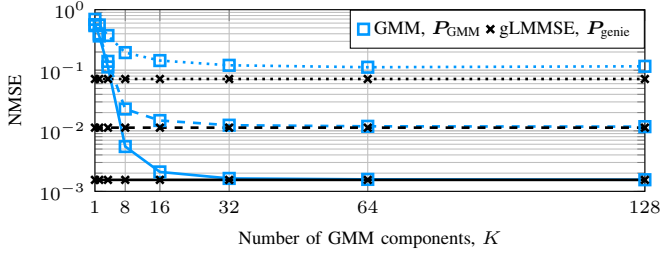


Fig. 5: The NMSE over the number of components  $K = 2^B$  for a MISO system ( $N_{\text{tx}} = 64$ ,  $N_{\text{rx}} = 1$ ) with  $n_p = 16$  pilots, for different SNR levels (dotted: 0 dB, dashed: 10 dB, solid: 20 dB).

components, a saturation can be observed. These results suggest that varying the number of GMM components  $K$ , allows for a performance-to-complexity trade-off without sacrificing too much in performance for  $K \geq 16$  components.

### B. Multi-user MIMO

In the following multi-user simulations, the performance is measured by the NMSE averaged over the number of MTs  $J$  and  $M_{\text{con}} = 500$  constellations, with  $J$  MTs randomly drawn from our evaluation set for each constellation. If not mentioned otherwise, we consider the block with index  $t = 5$  in the simulations, do not specify a maximum number of iterations  $L_{\text{max}}$  for the pilot optimization algorithm (Algorithm 1) from Section IV-A, and initialize with a random pilot matrix.

In Fig. 6, we consider a MU-MIMO system, with  $J = 4$  MTs,  $N_{\text{tx}} = 32$  BS antennas,  $N_{\text{rx}} = 4$  MT antennas, and  $n_p = 8$  pilots. Due to the MIMO setup, we fit a Kronecker-structured GMM with in total  $K = 2^7 = 128$  components ( $B = 7$  feedback bits per MT), where  $K_{\text{tx}} = 32$  and  $K_{\text{rx}} = 4$ . The proposed GMM-based pilot design approach “GMM,  $\mathbf{P}_{\text{GMM}}$ ” (see Section IV-C) outperforms the baselines “GMM,  $\{\mathbf{P}_{\text{DFT}}, \mathbf{P}_{\text{RND}}\}$ ” by a large margin, where the GMM estimator is used in combination with either random pilot matrices or a random selection of columns of the two times oversampled DFT matrix as the pilot matrix. The baselines “gLMMSE,  $\{\mathbf{P}_{\text{DFT}}, \mathbf{P}_{\text{RND}}\}$ ” assume that each MT has perfect statistical knowledge of its channel to apply the utopian genie LMMSE approach (6) for channel estimation in combination with random or DFT-based pilots as described above. The GMM-based scheme outperforms the baseline “gLMMSE,  $\mathbf{P}_{\text{DFT}}$ ” over the whole SNR range, and the baseline “gLMMSE,  $\mathbf{P}_{\text{RND}}$ ” for SNR values larger than 0 dB. In addition to the assumption of perfect statistical knowledge at each MT about its own channel, the baseline “gLMMSE,  $\mathbf{P}_{\text{genie}}$ ” further assumes perfect statistical knowledge of the channels of all MTs at the BS in order to design the pilot matrix using Algorithm 1 from Section IV-A. The GMM-based scheme performs only slightly worse than this utopian baseline. A larger gap is present in the low SNR regime, where the feedback information of each MT obtained through the responsibilities [see (30)] is less accurate due to high noise.

In Fig. 7, we analyze the performance of the GMM-based pilot design scheme over the block index  $t$  for the same MU-MIMO setup as before at three different SNR levels, i.e.,  $\text{SNR} \in \{0 \text{ dB}, 10 \text{ dB}, 20 \text{ dB}\}$ . As discussed in Section IV-C, at  $t = 0$ , we utilize a random selection of columns of the two times oversampled DFT matrix as the pilot matrix. Similar to

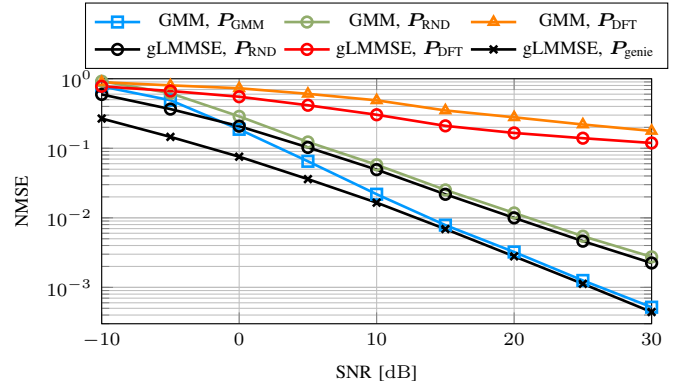


Fig. 6: The NMSE over the SNR for a MU-MIMO system ( $N_{\text{tx}} = 32$ ,  $N_{\text{rx}} = 4$ ) with  $J = 4$  MTs,  $B = 7$  feedback bits and  $n_p = 8$  pilots.

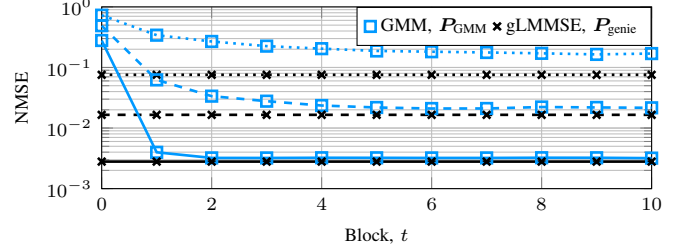


Fig. 7: The NMSE over the block index  $t$  for a MU-MIMO system ( $N_{\text{tx}} = 32$ ,  $N_{\text{rx}} = 4$ ) with  $J = 4$  MTs,  $B = 7$  feedback bits,  $n_p = 8$  pilots, for different SNR levels (dotted: 0 dB, dashed: 10 dB, solid: 20 dB).

the single-user case (see Fig. 3), after only one block, we can see a significant gain in performance of the proposed GMM-based pilot design scheme due to the feedback of the index of each MT. Additionally, with an increasing SNR, fewer blocks are required to achieve a performance close to the utopian baseline “gLMMSE,  $\mathbf{P}_{\text{genie}}$ ” which requires perfect statistical knowledge at the BS and the MTs.

In Fig. 8, for the same MU-MIMO system with  $n_p = 16$  pilots, the effect of using the iterative algorithm from [9] following Corollary 2.1 due to the established lower bound in Theorem 2 instead of the iterative approach (Algorithm 1) outlined in Section IV-A, subject to a maximum number of iterations  $L_{\text{max}}$ , is analyzed. Moreover, in addition to the initialization of the iterative algorithm with a random pilot matrix, we consider a random selection of columns of the two times oversampled DFT matrix as an alternative initially chosen pilot matrix. Accordingly, the curves labeled “ $\{\text{GMM, gLMMSE}\}, \mathbf{P}_{\text{GMM}}, \{\text{LB-RND, LB-DFT}\}$ ” utilize the lower bound maximization, with either random or DFT-based initialization using the GMM-based feedback scheme, or perfect statistical knowledge at the BS and the MTs, respectively. With “gLMMSE,  $\mathbf{P}_{\text{genie}}$ ,” we denote the baseline where the iterative algorithm from Section IV-A is used in combination with random initialization and no maximum number of iterations  $L_{\text{max}}$  being specified. In Fig. 8, we can see that for low values for  $L_{\text{max}}$ , a random initialization of the iterative lower-bound maximization is advantageous as compared to a DFT-based initialization, irrespective of whether we use the GMM-based scheme or require perfect statistical knowledge. For a high SNR value of 20 dB (solid), the DFT-based initialization requires larger values for  $L_{\text{max}}$  to achieve a similar performance as the random initialization. However, for the GMM-based scheme, where an information feedforward from the BS to

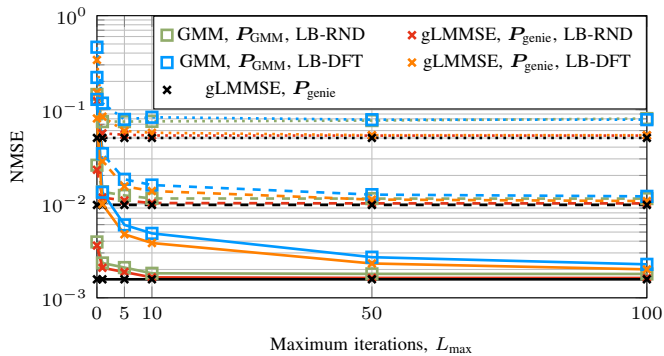


Fig. 8: The NMSE over the number of maximum iterations  $L_{\max}$  for a MU-MIMO system ( $N_{\text{tx}} = 32$ ,  $N_{\text{rx}} = 4$ ) with  $J = 4$  MTs,  $B = 7$  feedback bits, and  $n_p = 16$  pilots for different SNR levels (dotted: 0 dB, dashed: 10 dB, solid: 20 dB).

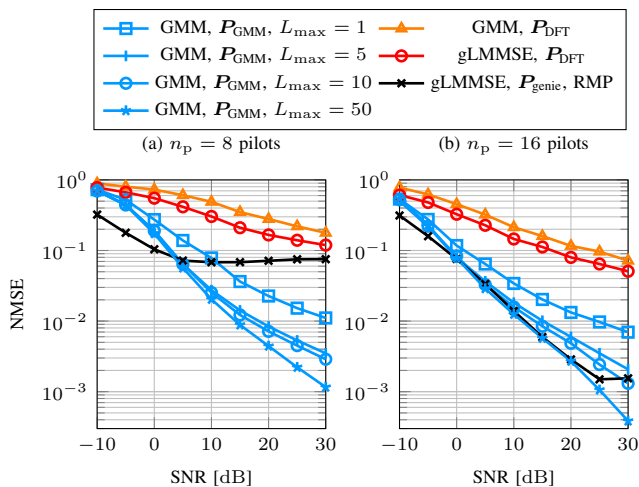


Fig. 9: The NMSE over the SNR for a MU-MIMO system ( $N_{\text{tx}} = 32$ ,  $N_{\text{rx}} = 4$ ) with  $J = 4$  MTs,  $B = 7$  feedback bits, and (a)  $n_p = 8$  pilots, or (b)  $n_p = 16$  pilots.

the MTs is required, DFT-based initialization is advantageous as it eliminates the need for seed exchange and a common random number generator between the BS and MTs, enhancing practicability. We can see further that for an SNR of 0 dB (dotted), there is a gap present between the GMM-based scheme compared to the case where perfect statistical knowledge is required since the feedback information of each MT obtained through the responsibilities given an observation [see (30)] is less accurate due to high noise. We have observed this behavior for different numbers of pilots  $n_p$ . Overall, this analysis suggests that with the lower bound maximization using the iterative algorithm from [9] following Corollary 2.1, together with a relatively low number of maximum iterations  $L_{\max}$ , a pilot matrix design of relatively low complexity is possible without sacrificing too much performance. In the next simulations, we focus our analysis on DFT-based initialization due to superior practicability compared to random initialization.

In Fig. 9(a) and Fig. 9(b), we again consider the MU-MIMO setup from before, with  $n_p = 8$  pilots or  $n_p = 16$  pilots, respectively. The proposed GMM-based pilot design approaches labeled “GMM,  $\mathbf{P}_{\text{GMM}}$ ,  $L_{\max} \in \{1, 5, 10, 50\}$ ” utilize the lower-bound maximization by using the iterative algorithm from [9] following Corollary 2.1 together with DFT-based initialization with different maximum numbers of iterations  $L_{\max}$ . We can observe that even one iteration ( $L_{\max} = 1$ ) is enough to outperform the baselines “{GMM, gLMMSE},

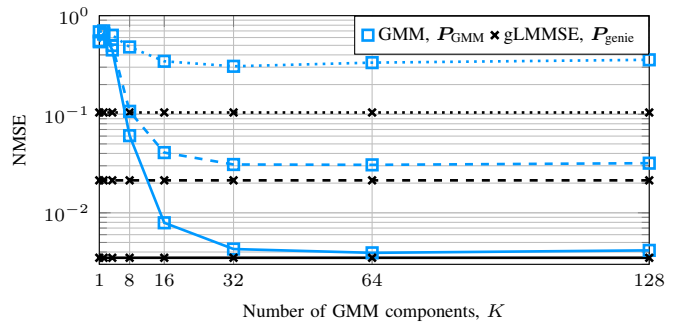


Fig. 10: The NMSE over the number of components  $K = 2^B$  for a MU-MISO system ( $N_{\text{tx}} = 64$ ,  $N_{\text{rx}} = 1$ ) with  $J = 8$  MTs,  $n_p = 16$  pilots, for different SNR levels (dotted: 0 dB, dashed: 10 dB, solid: 20 dB).

$\mathbf{P}_{\text{DFT}}$ ,” by a large margin. In Fig. 9(a), for SNR values larger than approximately 5 dB and even  $L_{\max} = 5$ , the proposed scheme even outperforms “gLMMSE,  $\mathbf{P}_{\text{genie}}$ , RMP,” i.e., the state-of-the-art pilot matrix signaling scheme from Section IV-B with  $B_{\text{RMP}} = 7$  bits; there, each MT has perfect statistical knowledge of its channel to apply the utopian genie LMMSE approach from (6) for channel estimation, and perfect statistical knowledge of the channels of all MTs at the BS is assumed to design the pilot matrix using the iterative algorithm from Section IV-A prior to quantization with the RMP algorithm. The error floor with the RMP-based scheme was already similarly observed and discussed in [10]. In Fig. 9(b), with  $n_p = 16$  pilots, the error floor of the RMP-based scheme is present for SNR values larger than 25 dB. The proposed GMM-based scheme, which does not require any *a priori* statistics, performs very well also in this setup. Note that in these particular setups, the RMP-based scheme requires in total  $n_p B_{\text{RMP}}$  feedforward bits, yielding 56 bits for the setup in Fig. 9(a), and 112 bits for the setup in Fig. 9(b), whereas the GMM-based scheme does not depend on the number of pilots  $n_p$  and only requires in total  $JB = 28$  feedforward bits.

Lastly, in Fig. 10, we analyze the effect of varying the number of GMM-components  $K$  on the scheme’s performance in a MU-MISO system with  $J = 8$  single-antenna MTs and  $N_{\text{tx}} = 64$  BS antennas. We set  $n_p = 16$  pilots and consider three different SNR levels, i.e.,  $\text{SNR} \in \{0 \text{ dB}, 10 \text{ dB}, 20 \text{ dB}\}$ . Since we consider single-antenna MTs in this setup, we apply the iterative algorithm from [9], utilize DFT-based initialization, and set the maximum number of iterations  $L_{\max} = 50$ , with the GMM-based scheme. For the “gLMMSE,  $\mathbf{P}_{\text{genie}}$ ” baseline, random initialization is applied, and no maximum number of iterations  $L_{\max}$  is specified. Similar to the single-user case in Fig. 5, we can observe that the estimation error decreases with an increasing number of components  $K$ . With an increasing SNR, the gap to the genie-aided approach “gLMMSE,  $\mathbf{P}_{\text{genie}}$ ” decreases. Compared to the single-user case, slightly more GMM-components are needed in a multi-user system. An intuitive explanation is that with the GMM-based scheme, the true but unknown covariance of each MT is approximated, and the approximation error accumulates over multiple MTs. With more components, the approximation error decreases, yielding a better performance. Overall, also in the multi-user case, these results suggest that a performance-to-complexity trade-off can be realized by varying the number of GMM components  $K$ .

## IX. CONCLUSION

In this work, we proposed a GMM-based pilot design scheme for single- and multi-user MIMO FDD systems. A significant advantage of the proposed scheme is that it does not require *a priori* knowledge of the channel's statistics at the BS and the MTs. Instead, it relies on a feedback mechanism, establishing common knowledge of the pilot matrix in a single-user system. In the multi-user case, the pilot design involves an additional feedforward of the indices of the GMM components. The GMM-based scheme offers significant versatility since it can generally be adapted to any desired SNR level, pilot configuration, and different numbers of MTs without requiring re-training. Simulation results show that the performance gains achieved with the proposed scheme allow the deployment of system setups with reduced pilot overhead while maintaining a similar estimation performance. In future work, the extension of the GMM-based pilot scheme to systems with a spatio-temporal correlation of channels [10], [46], [47] can be investigated.

## APPENDIX

### A. Proof of Theorem 1

We start by rewriting the sum CMI expression in (18) by utilizing for all  $j \in \mathcal{J}$ ,  $\mathbf{C}_{\delta_j} = \mathbf{C}_{\delta_j}^{\text{tx}} \otimes \mathbf{C}_{\delta_j}^{\text{rx}}$ , and the Kronecker product rules (see [48]) as

$$\begin{aligned} & \sum_{j=1}^J \log \det \left( \mathbf{I} + \frac{1}{\sigma_n^2} (\mathbf{P}_t \otimes \mathbf{I}_{N_{\text{rx}}}) \mathbf{C}_{\delta_j} (\mathbf{P}_t \otimes \mathbf{I}_{N_{\text{rx}}})^{\text{H}} \right) \\ &= \sum_{j=1}^J \log \det \left( \mathbf{I} + \frac{1}{\sigma_n^2} (\mathbf{P}_t \mathbf{C}_{\delta_j}^{\text{tx}} \mathbf{P}_t^{\text{H}}) \otimes \mathbf{C}_{\delta_j}^{\text{rx}} \right). \end{aligned} \quad (32)$$

The partial derivative of the sum CMI with respect to the entry of the conjugate of the pilot matrix  $[\mathbf{P}_t^*]_{r,c}$  at row  $r$  and column  $c$  is then given by

$$\begin{aligned} & \frac{\partial}{\partial [\mathbf{P}_t^*]_{r,c}} \left( \sum_{j=1}^J \log \det \left( \mathbf{I} + \frac{1}{\sigma_n^2} (\mathbf{P}_t \mathbf{C}_{\delta_j}^{\text{tx}} \mathbf{P}_t^{\text{H}}) \otimes \mathbf{C}_{\delta_j}^{\text{rx}} \right) \right) \\ &= \sum_{j=1}^J \text{tr} \left( \left( \mathbf{I} + \frac{1}{\sigma_n^2} (\mathbf{P}_t \mathbf{C}_{\delta_j}^{\text{tx}} \mathbf{P}_t^{\text{H}}) \otimes \mathbf{C}_{\delta_j}^{\text{rx}} \right)^{-1} \right. \\ & \quad \left. \times \frac{\partial}{\partial [\mathbf{P}_t^*]_{r,c}} \left( \mathbf{I} + \frac{1}{\sigma_n^2} (\mathbf{P}_t \mathbf{C}_{\delta_j}^{\text{tx}} \mathbf{P}_t^{\text{H}}) \otimes \mathbf{C}_{\delta_j}^{\text{rx}} \right) \right) \end{aligned} \quad (33)$$

$$\begin{aligned} &= \sum_{j=1}^J \text{tr} \left( \left( \mathbf{I} + \frac{1}{\sigma_n^2} (\mathbf{P}_t \mathbf{C}_{\delta_j}^{\text{tx}} \mathbf{P}_t^{\text{H}}) \otimes \mathbf{C}_{\delta_j}^{\text{rx}} \right)^{-1} \right. \\ & \quad \left. \times \left( \frac{1}{\sigma_n^2} (\mathbf{P}_t \mathbf{C}_{\delta_j}^{\text{tx}} \mathbf{e}_c \mathbf{e}_r^{\text{T}}) \otimes \mathbf{C}_{\delta_j}^{\text{rx}} \right) \right), \end{aligned} \quad (34)$$

where (33) follows from the linearity of the sum, and using the derivation rule provided in [49, eq. (46)]. By utilizing the SVDs

$$\mathbf{P}_t \mathbf{C}_{\delta_j}^{\text{tx}} \mathbf{P}_t^{\text{H}} = \mathbf{V}_j \mathbf{S}_j \mathbf{V}_j^{\text{H}}, \quad (35)$$

$$\mathbf{C}_{\delta_j}^{\text{rx}} = \mathbf{W}_j \mathbf{T}_j \mathbf{W}_j^{\text{H}}, \quad (36)$$

using  $\mathbf{I} = (\mathbf{V}_j \otimes \mathbf{W}_j)(\mathbf{V}_j \otimes \mathbf{W}_j)^{\text{H}}$ , and applying basic Kronecker product rules, we have that

$$\begin{aligned} & \left( \mathbf{I} + \frac{1}{\sigma_n^2} (\mathbf{P}_t \mathbf{C}_{\delta_j}^{\text{tx}} \mathbf{P}_t^{\text{H}}) \otimes \mathbf{C}_{\delta_j}^{\text{rx}} \right)^{-1} \\ &= (\mathbf{V}_j \otimes \mathbf{W}_j) \left( \mathbf{I} + \frac{1}{\sigma_n^2} \mathbf{S}_j \otimes \mathbf{T}_j \right)^{-1} (\mathbf{V}_j \otimes \mathbf{W}_j)^{\text{H}}. \end{aligned} \quad (37)$$

Note that  $\mathbf{S}_j \otimes \mathbf{T}_j$  is diagonal. Let  $\sum_{i=1}^I \alpha_{j,i} \gamma_{j,i} \beta_{j,i}^{\text{T}}$  with  $I = \min(n_p, N_{\text{rx}})$ , be the SVD of the matrix  $\text{unvec}_{N_{\text{rx}}, n_p} \left( \text{diag} \left( \left( \mathbf{I} + \frac{1}{\sigma_n^2} \mathbf{S}_j \otimes \mathbf{T}_j \right)^{-1} \right) \right)$  for all  $j \in \mathcal{J}$ . Then, it holds for all  $j \in \mathcal{J}$ ,

$$\begin{aligned} & \left( \mathbf{I} + \frac{1}{\sigma_n^2} \mathbf{S}_j \otimes \mathbf{T}_j \right)^{-1} \\ &= \sum_{i=1}^I \text{diag}(\alpha_{j,i} \beta_{j,i} \otimes \gamma_{j,i}) = \sum_{i=1}^I \mathbf{D}_{\beta_{j,i}} \otimes \mathbf{D}_{\gamma_{j,i}}, \end{aligned} \quad (38)$$

which are real-valued Kronecker product SVDs, see [50], with the integer factorization of  $n_p$  and  $N_{\text{rx}}$ . Accordingly, the diagonal matrices  $\mathbf{D}_{\beta_{j,i}} \in \mathbb{R}^{n_p \times n_p}$  and  $\mathbf{D}_{\gamma_{j,i}} \in \mathbb{R}^{N_{\text{rx}} \times N_{\text{rx}}}$  for all  $j \in \mathcal{J}$ , are defined as  $\mathbf{D}_{\beta_{j,i}} = \alpha_{j,i} \text{diag}(\beta_{j,i})$  and  $\mathbf{D}_{\gamma_{j,i}} = \text{diag}(\gamma_{j,i})$ . Note that the specific dimensions (the integer factorization of  $n_p$  and  $N_{\text{rx}}$ ) are required to proceed with simplifications involving Kronecker products. Incorporating (37) and (38) into (34), we obtain

$$\begin{aligned} & \sum_{j=1}^J \text{tr} \left( (\mathbf{V}_j \otimes \mathbf{W}_j) \left( \sum_{i=1}^I \mathbf{D}_{\beta_{j,i}} \otimes \mathbf{D}_{\gamma_{j,i}} \right) (\mathbf{V}_j \otimes \mathbf{W}_j)^{\text{H}} \right. \\ & \quad \left. \times \left( \frac{1}{\sigma_n^2} (\mathbf{P}_t \mathbf{C}_{\delta_j}^{\text{tx}} \mathbf{e}_c \mathbf{e}_r^{\text{T}}) \otimes \mathbf{C}_{\delta_j}^{\text{rx}} \right) \right), \end{aligned} \quad (39)$$

which can be further reformulated by exploiting (36), basic Kronecker product and trace rules to

$$\begin{aligned} & \sum_{j=1}^J \text{tr} \left( \left( \sum_{i=1}^I \mathbf{D}_{\beta_{j,i}} \otimes \mathbf{D}_{\gamma_{j,i}} \right) \right. \\ & \quad \left. \times \left( \frac{1}{\sigma_n^2} (\mathbf{V}_j^{\text{H}} \mathbf{P}_t \mathbf{C}_{\delta_j}^{\text{tx}} \mathbf{e}_c \mathbf{e}_r^{\text{T}} \mathbf{V}_j) \otimes \mathbf{T}_j \right) \right) \\ &= \sum_{j=1}^J \text{tr} \left( \sum_{i=1}^I \left( \frac{1}{\sigma_n^2} (\mathbf{D}_{\beta_{j,i}} \mathbf{V}_j^{\text{H}} \mathbf{P}_t \mathbf{C}_{\delta_j}^{\text{tx}} \mathbf{e}_c \mathbf{e}_r^{\text{T}} \mathbf{V}_j) \otimes (\mathbf{D}_{\gamma_{j,i}} \mathbf{T}_j) \right) \right) \end{aligned} \quad (40)$$

$$\begin{aligned} &= \sum_{j=1}^J \sum_{i=1}^I \text{tr} \left( \frac{1}{\sigma_n^2} \mathbf{D}_{\beta_{j,i}} \mathbf{V}_j^{\text{H}} \mathbf{P}_t \mathbf{C}_{\delta_j}^{\text{tx}} \mathbf{e}_c \mathbf{e}_r^{\text{T}} \mathbf{V}_j \right) \text{tr}(\mathbf{D}_{\gamma_{j,i}} \mathbf{T}_j) \end{aligned} \quad (41)$$

$$\begin{aligned} &= \sum_{j=1}^J \sum_{i=1}^I \frac{1}{\sigma_n^2} \mathbf{e}_r^{\text{T}} \mathbf{V}_j \mathbf{D}_{\beta_{j,i}} \mathbf{V}_j^{\text{H}} \mathbf{P}_t \mathbf{C}_{\delta_j}^{\text{tx}} \mathbf{e}_c \text{tr}(\mathbf{D}_{\gamma_{j,i}} \mathbf{T}_j). \end{aligned} \quad (42)$$

Accordingly, it holds:

$$\begin{aligned} & \frac{\partial}{\partial \mathbf{P}_t^*} \left( \sum_{j=1}^J \log \det \left( \mathbf{I} + \frac{1}{\sigma_n^2} (\mathbf{P}_t \mathbf{C}_{\delta_j}^{\text{tx}} \mathbf{P}_t^{\text{H}}) \otimes \mathbf{C}_{\delta_j}^{\text{rx}} \right) \right) \\ &= \sum_{j=1}^J \sum_{i=1}^I \frac{1}{\sigma_n^2} \mathbf{V}_j \mathbf{D}_{\beta_{j,i}} \mathbf{V}_j^{\text{H}} \mathbf{P}_t \mathbf{C}_{\delta_j}^{\text{tx}} \text{tr}(\mathbf{D}_{\gamma_{j,i}} \mathbf{T}_j). \end{aligned} \quad (43)$$

It remains to set the derivative of the dual function of the optimization problem (18) with respect to  $\mathbf{P}_t^*$  to zero to observe the first-order necessary KKT condition provided in (19), cf., e.g., [51].

### B. Proof of Theorem 2

Given the reformulated sum CMI expression from (32) and by using (35) and (36), the sum CMI can be expressed as

$$\begin{aligned} & \sum_{j=1}^J \log \det \left( \mathbf{I} + \frac{1}{\sigma_n^2} \mathbf{S}_j \otimes \mathbf{T}_j \right) \\ &= \sum_{j=1}^J \log \det \left( \mathbf{I} + \frac{1}{\sigma_n^2} \text{tr}(\mathbf{T}_j) \mathbf{S}_j \otimes \frac{1}{\text{tr}(\mathbf{T}_j)} \mathbf{T}_j \right). \end{aligned} \quad (44)$$

By further defining for all  $j \in \mathcal{J}$ ,  $\frac{1}{\text{tr}(\mathbf{T}_j)} \mathbf{T}_j = \sum_{i=1}^{N_{\text{rx}}} t_{j,i} \text{diag}(\mathbf{e}_i)$  with  $\sum_{i=1}^{N_{\text{rx}}} t_{j,i} = 1$ , we can rewrite the expression provided in (44) and lower bound it using the concavity of the log-determinant expression (see [52, Th. 7.6.6]) as

$$\begin{aligned} & \sum_{j=1}^J \log \det \left( \mathbf{I} + \frac{1}{\sigma_n^2} \text{tr}(\mathbf{T}_j) \mathbf{S}_j \otimes \left( \sum_i t_{j,i} \text{diag}(\mathbf{e}_i) \right) \right) \\ &= \sum_{j=1}^J \log \det \sum_i t_{j,i} \left( \mathbf{I} + \frac{1}{\sigma_n^2} \text{tr}(\mathbf{T}_j) \mathbf{S}_j \otimes \text{diag}(\mathbf{e}_i) \right) \end{aligned} \quad (45)$$

$$\geq \sum_{j=1}^J \sum_{i=1}^{N_{\text{rx}}} t_{j,i} \log \det \left( \mathbf{I} + \frac{1}{\sigma_n^2} \text{tr}(\mathbf{T}_j) \mathbf{S}_j \otimes \text{diag}(\mathbf{e}_i) \right) \quad (46)$$

$$= \sum_{j=1}^J \sum_{i=1}^{N_{\text{rx}}} t_{j,i} \log \det \left( \mathbf{I} + \frac{1}{\sigma_n^2} \text{tr}(\mathbf{T}_j) \mathbf{S}_j \right) \quad (47)$$

$$= \sum_{j=1}^J \log \det \left( \mathbf{I} + \frac{1}{\sigma_n^2} \text{tr}(\mathbf{T}_j) \mathbf{S}_j \right). \quad (48)$$

Since  $\text{tr}(\mathbf{C}_{\delta_j}^{\text{rx}}) = \text{tr}(\mathbf{T}_j)$ , see (36), and by incorporating (35) in (26), and using  $\mathbf{I} = \mathbf{V}_j \mathbf{V}_j^{\text{H}}$ , yields (48), finishing the proof.

### C. Proof of Proposition 2.1

Observe that the inequality in (46) becomes an equality if for all  $j \in \mathcal{J}$  and any  $i', t_{j,i'} = 1 \wedge t_{j,i} = 0$  for all  $i \neq i'$ , i.e.,  $\text{rk}(\mathbf{C}_{\delta_j}^{\text{rx}}) = 1$  for all  $j \in \mathcal{J}$ . In any other case, if there is at least one MT  $j$  for which  $\text{rk}(\mathbf{C}_{\delta_j}^{\text{rx}}) > 1$  holds with accordingly  $t_{j,i} \in (0, 1)$  for all  $i$ , and since then

$$\mathbf{I} + \frac{1}{\sigma_n^2} \text{tr}(\mathbf{T}_j) \mathbf{S}_j \otimes \text{diag}(\mathbf{e}_i) \neq \mathbf{I} + \frac{1}{\sigma_n^2} \text{tr}(\mathbf{T}_j) \mathbf{S}_j \otimes \text{diag}(\mathbf{e}_{i'}) \quad (49)$$

due to the structure of the resulting matrices for  $i \neq i'$ , the condition for equality between (45) and (46) according to [52, Th. 7.6.6] is not met (equality in (49) is required).

### D. Proof of Proposition 2.2

The lower bound expression from (26) only depends on the trace of each MTs receive-side covariance matrix  $\mathbf{C}_{\delta_j}^{\text{rx}}$  for all  $j \in \mathcal{J}$ . We outline next that the sum CMI attains its largest value and consequently exhibits the largest gap to the lower

bound for the case of no spatial correlation for all  $j \in \mathcal{J}$ . Thus, given the reformulated sum CMI from (44), we have to show

$$\begin{aligned} & \sum_{j=1}^J \log \det \left( \mathbf{I} + \frac{1}{\sigma_n^2} \tau_j \mathbf{S}_j \otimes \frac{1}{N_{\text{rx}}} \mathbf{I} \right) \\ & \stackrel{!}{>} \sum_{j=1}^J \log \det \left( \mathbf{I} + \frac{1}{\sigma_n^2} \tau_j \mathbf{S}_j \otimes \frac{1}{N_{\text{rx}}} (\mathbf{I} + \text{diag}(\boldsymbol{\kappa}_j)) \right), \end{aligned} \quad (50)$$

where for all  $j \in \mathcal{J}$ , the elements of  $\boldsymbol{\kappa}_j$  satisfy  $\sum_{\ell=1}^{N_{\text{rx}}} \kappa_{j,\ell} = 0$ , with  $\kappa_{j,\ell} + 1 \geq 0$ , and  $\boldsymbol{\kappa}_j \neq \mathbf{0}$  (in this way, for all  $j \in \mathcal{J}$ , the eigenvalues of any valid receive-side covariance matrix, except the weighted identity, are parametrized). Since the involved matrices are diagonal, we have

$$\begin{aligned} & \sum_{j=1}^J \log \prod_{i=1}^{n_p} \left( 1 + \frac{\tau_j}{\sigma_n^2 N_{\text{rx}}} s_{j,i} \right)^{N_{\text{rx}}} \\ & \stackrel{!}{>} \sum_{j=1}^J \log \prod_{i=1}^{n_p} \prod_{\ell=1}^{N_{\text{rx}}} \left( 1 + \frac{\tau_j}{\sigma_n^2 N_{\text{rx}}} s_{j,i} (1 + \kappa_{j,\ell}) \right), \end{aligned} \quad (51)$$

which can be further rewritten to

$$\begin{aligned} & \sum_{j=1}^J \sum_{i=1}^{n_p} \log \left( 1 + \frac{\tau_j}{\sigma_n^2 N_{\text{rx}}} s_{j,i} \right)^{N_{\text{rx}}} \\ & \stackrel{!}{>} \sum_{j=1}^J \sum_{i=1}^{n_p} \sum_{\ell=1}^{N_{\text{rx}}} \log \left( 1 + \frac{\tau_j}{\sigma_n^2 N_{\text{rx}}} s_{j,i} (1 + \kappa_{j,\ell}) \right). \end{aligned} \quad (52)$$

For a fixed  $j$  and  $i$ , we thus have to show

$$N_{\text{rx}} \log \left( 1 + \frac{\tau_j}{\sigma_n^2 N_{\text{rx}}} s_{j,i} \right) \stackrel{!}{>} \sum_{\ell=1}^{N_{\text{rx}}} \log \left( 1 + \frac{\tau_j}{\sigma_n^2 N_{\text{rx}}} s_{j,i} (1 + \kappa_{j,\ell}) \right), \quad (53)$$

which can be reformulated by dividing both sides by  $N_{\text{rx}}$  as

$$\begin{aligned} & \log \left( \sum_{\ell=1}^{N_{\text{rx}}} \frac{1}{N_{\text{rx}}} \left( 1 + \frac{\tau_j}{\sigma_n^2 N_{\text{rx}}} s_{j,i} \right) \right) \\ & \stackrel{!}{>} \sum_{\ell=1}^{N_{\text{rx}}} \frac{1}{N_{\text{rx}}} \log \left( 1 + \frac{\tau_j}{\sigma_n^2 N_{\text{rx}}} s_{j,i} (1 + \kappa_{j,\ell}) \right). \end{aligned} \quad (54)$$

Observing that the expression provided in (55) is equal to (54) and the following inequality is true due to Jensen's inequality

$$\begin{aligned} & \log \left( \sum_{\ell=1}^{N_{\text{rx}}} \frac{1}{N_{\text{rx}}} \left( 1 + \frac{\tau_j}{\sigma_n^2 N_{\text{rx}}} s_{j,i} (1 + \kappa_{j,\ell}) \right) \right) \\ & > \sum_{\ell=1}^{N_{\text{rx}}} \frac{1}{N_{\text{rx}}} \log \left( 1 + \frac{\tau_j}{\sigma_n^2 N_{\text{rx}}} s_{j,i} (1 + \kappa_{j,\ell}) \right), \end{aligned} \quad (55)$$

and is strict since  $\boldsymbol{\kappa}_j \neq \mathbf{0}$ , the only condition for which equality can hold is not satisfied, i.e.  $1 + \frac{\tau_j}{\sigma_n^2 N_{\text{rx}}} s_{j,i} (1 + \kappa_{j,\ell}) \neq 1 + \frac{\tau_j}{\sigma_n^2 N_{\text{rx}}} s_{j,i} (1 + \kappa_{j,\ell'})$  for  $\ell \neq \ell'$ .

## REFERENCES

- [1] N. Turan, B. Fesl, B. Böck, M. Joham, and W. Utschick, "Channel-adaptive pilot design for FDD-MIMO systems utilizing Gaussian mixture models," in *Int. Symp. Wireless Commun. Syst. (ISWCS)*, 2024, to be published, arXiv preprint: 2403.17577.

- [2] E. Björnson, L. Sanguinetti, H. Wymeersch, J. Hoydis, and T. L. Marzetta, "Massive MIMO is a reality—What is next? five promising research directions for antenna arrays," *Digit. Signal Process.*, vol. 94, pp. 3–20, 2019, Special Issue on Source Localization in Massive MIMO.
- [3] E. Björnson, E. G. Larsson, and T. L. Marzetta, "Massive MIMO: ten myths and one critical question," *IEEE Commun. Mag.*, vol. 54, no. 2, pp. 114–123, 2016.
- [4] J. Choi, D. J. Love, and P. Bidigare, "Downlink training techniques for FDD massive MIMO systems: Open-loop and closed-loop training with memory," *IEEE J. Sel. Areas Commun.*, vol. 8, no. 5, pp. 802–814, 2014.
- [5] J. Kotecha and A. Sayeed, "Transmit signal design for optimal estimation of correlated MIMO channels," *IEEE Trans. Signal Process.*, vol. 52, no. 2, pp. 546–557, 2004.
- [6] E. Björnson and B. Ottersten, "A framework for training-based estimation in arbitrarily correlated Rician MIMO channels with Rician disturbance," *IEEE Trans. Signal Process.*, vol. 58, no. 3, pp. 1807–1820, 2010.
- [7] J. Pang, J. Li, L. Zhao, and Z. Lu, "Optimal training sequences for MIMO channel estimation with spatial correlation," in *IEEE 66th Veh. Technol. Conf.*, 2007, pp. 651–655.
- [8] J. Fang, X. Li, H. Li, and F. Gao, "Low-rank covariance-assisted downlink training and channel estimation for FDD massive MIMO systems," *IEEE Trans. Wireless Commun.*, vol. 16, no. 3, pp. 1935–1947, 2017.
- [9] Z. Jiang, A. F. Molisch, G. Caire, and Z. Niu, "Achievable rates of FDD massive MIMO systems with spatial channel correlation," *IEEE Trans. Wireless Commun.*, vol. 14, no. 5, pp. 2868–2882, 2015.
- [10] S. Bazzi and W. Xu, "Downlink training sequence design for FDD multiuser massive MIMO systems," *IEEE Trans. Signal Process.*, vol. 65, no. 18, pp. 4732–4744, 2017.
- [11] Y. Gu and Y. D. Zhang, "Information-theoretic pilot design for downlink channel estimation in FDD massive MIMO systems," *IEEE Trans. Signal Process.*, vol. 67, no. 9, pp. 2334–2346, 2019.
- [12] D. Guo, S. Shamai, and S. Verdú, "Mutual information and minimum mean-square error in Gaussian channels," *IEEE Trans. Inf. Theory*, vol. 51, no. 4, pp. 1261–1282, 2005.
- [13] X. Ma and Z. Gao, "Data-driven deep learning to design pilot and channel estimator for massive MIMO," *IEEE Trans. Veh. Technol.*, vol. 69, no. 5, pp. 5677–5682, 2020.
- [14] M. B. Mashhadi and D. Gündüz, "Pruning the pilots: Deep learning-based pilot design and channel estimation for MIMO-OFDM systems," *IEEE Trans. Wireless Commun.*, vol. 20, no. 10, pp. 6315–6328, 2021.
- [15] I. Goodfellow, J. Pouget-Abadie, M. Mirza, B. Xu, D. Warde-Farley, S. Ozair, A. Courville, and Y. Bengio, "Generative adversarial nets," in *Proc. Adv. Neural Inf. Process. Syst.*, 2014, pp. 2672–2680.
- [16] D. P. Kingma and M. Welling, "Auto-encoding variational Bayes," in *Proc. Int. Conf. Learn. Representations (ICLR)*, 2014.
- [17] J. Ho, A. Jain, and P. Abbeel, "Denoising diffusion probabilistic models," in *Proc. 34th Int. Conf. Neural Inf. Process. Syst.*, 2020, pp. 6840–6851.
- [18] E. Balevi, A. Doshi, A. Jalal, A. Dimakis, and J. G. Andrews, "High dimensional channel estimation using deep generative networks," *IEEE J. Sel. Areas Commun.*, vol. 39, no. 1, pp. 18–30, 2021.
- [19] Y. Li, K. Li, L. Cheng, Q. Shi, and Z.-Q. Luo, "Digital twin-aided learning to enable robust beamforming: Limited feedback meets deep generative models," in *IEEE 22nd Int. Workshop on Signal Process. Advances in Wireless Commun. (SPAWC)*, 2021, pp. 26–30.
- [20] H. Ye, L. Liang, G. Y. Li, and B.-H. Juang, "Deep learning-based end-to-end wireless communication systems with conditional GANs as unknown channels," *IEEE Trans. Wireless Commun.*, vol. 19, no. 5, pp. 3133–3143, 2020.
- [21] M. Kim, R. Fritschek, and R. F. Schaefer, "Learning end-to-end channel coding with diffusion models," in *WSA & SCC: 26th Int. ITG Workshop Smart Antennas and 13th Conf. Syst., Commun., Coding*, 2023, pp. 1–6.
- [22] P. Mukherjee, D. Mishra, and S. De, "Gaussian mixture based context-aware short-term characterization of wireless channels," *IEEE Trans. Veh. Technol.*, vol. 69, no. 1, pp. 26–40, 2020.
- [23] Y. Li, J. Zhang, Z. Ma, and Y. Zhang, "Clustering analysis in the wireless propagation channel with a variational Gaussian mixture model," *IEEE Trans. Big Data*, vol. 6, no. 2, pp. 223–232, 2020.
- [24] Y. Gu and Y. D. Zhang, "Information-theoretic pilot design for downlink channel estimation in FDD massive MIMO systems," *IEEE Trans. Signal Process.*, vol. 67, no. 9, pp. 2334–2346, 2019.
- [25] M. Koller, B. Fesl, N. Turan, and W. Utschick, "An asymptotically MSE-optimal estimator based on Gaussian mixture models," *IEEE Trans. Signal Process.*, vol. 70, pp. 4109–4123, 2022.
- [26] N. Turan, B. Böck, K. J. Chan, B. Fesl, F. Burmeister, M. Joham, G. Fettweis, and W. Utschick, "Wireless channel prediction via Gaussian mixture models," in *27th Int. Workshop Smart Antennas (WSA)*, 2024, pp. 1–5.
- [27] N. Turan, B. Fesl, M. Koller, M. Joham, and W. Utschick, "A versatile low-complexity feedback scheme for FDD systems via generative modeling," *IEEE Trans. Wireless Commun.*, vol. 23, no. 6, pp. 6251–6265, 2024.
- [28] T. T. Nguyen, H. D. Nguyen, F. Chamroukhi, and G. J. McLachlan, "Approximation by finite mixtures of continuous density functions that vanish at infinity," *Cogent Math. Statist.*, vol. 7, no. 1, p. 1750861, 2020.
- [29] J. G. Andrews, S. Buzzi, W. Choi, S. V. Hanly, A. Lozano, A. C. K. Soong, and J. C. Zhang, "What will 5G be?" *IEEE J. Sel. Areas Commun.*, vol. 32, no. 6, pp. 1065–1082, 2014.
- [30] D. Neumann, T. Wiese, and W. Utschick, "Learning the MMSE channel estimator," *IEEE Trans. Signal Process.*, vol. 66, no. 11, pp. 2905–2917, Jun. 2018.
- [31] 3GPP, "Spatial channel model for multiple input multiple output (MIMO) simulations," 3rd Generation Partnership Project (3GPP), Tech. Rep. 25.996 (V16.0.0), Jul. 2020.
- [32] J. Kermaol, L. Schumacher, K. Pedersen, P. Mogensen, and F. Frederiksen, "A stochastic MIMO radio channel model with experimental validation," *IEEE J. Sel. Areas Commun.*, vol. 20, no. 6, pp. 1211–1226, 2002.
- [33] B. Fesl, N. Turan, B. Böck, and W. Utschick, "Channel estimation for quantized systems based on conditionally Gaussian latent models," *IEEE Trans. Signal Process.*, vol. 72, pp. 1475–1490, 2024.
- [34] N. Turan, B. Fesl, M. Grundei, M. Koller, and W. Utschick, "Evaluation of a Gaussian mixture model-based channel estimator using measurement data," in *Int. Symp. Wireless Commun. Syst. (ISWCS)*, 2022, pp. 1–6.
- [35] N. Turan, B. Fesl, M. Joham, Z. Ma, A. C. K. Soong, B. Sheen, W. Xiao, and W. Utschick, "Limited feedback on measurements: Sharing a codebook or a generative model?" in *IEEE 99th Veh. Technol. Conf. (VTC Spring)*, 2024, to be published, arXiv preprint: 2401.01721.
- [36] A. Alkhateeb, "DeepMIMO: A generic deep learning dataset for millimeter wave and massive MIMO applications," in *Proc. Inf. Theory Appl. Workshop (ITA)*, San Diego, CA, Feb 2019, pp. 1–8.
- [37] B. Böck, M. Baur, N. Turan, D. Semmler, and W. Utschick, "A statistical characterization of wireless channels conditioned on side information," 2024, arXiv: 2406.04282.
- [38] C. M. Bishop, *Pattern Recognition and Machine Learning (Information Science and Statistics)*. Berlin, Heidelberg: Springer-Verlag, 2006.
- [39] B. Fesl, M. Joham, S. Hu, M. Koller, N. Turan, and W. Utschick, "Channel estimation based on Gaussian mixture models with structured covariances," in *56th Asilomar Conf. Signals, Syst., Comput.*, 2022, pp. 533–537.
- [40] N. Turan, B. Fesl, and W. Utschick, "Enhanced low-complexity FDD system feedback with variable bit lengths via generative modeling," in *57th Asilomar Conf. Signals, Syst., Comput.*, 2023, pp. 363–369.
- [41] S. Bazzi and W. Xu, "On the amount of downlink training in correlated massive MIMO channels," *IEEE Trans. Signal Process.*, vol. 66, no. 9, pp. 2286–2299, 2018.
- [42] M. Gharavi-Alkhansari and T. Huang, "A fast orthogonal matching pursuit algorithm," in *IEEE Int. Conf. on Acoust., Speech and Signal Process. (ICASSP)*, vol. 3, 1998, pp. 1389–1392.
- [43] A. Alkhateeb, G. Leus, and R. W. Heath, "Compressed sensing based multi-user millimeter wave systems: How many measurements are needed?" in *IEEE Int. Conf. Acoust., Speech Signal Process. (ICASSP)*, 2015, pp. 2909–2913.
- [44] J. Bergstra and Y. Bengio, "Random search for hyper-parameter optimization," *J. of Mach. Learn. Res.*, vol. 13, p. 281–305, Feb. 2012.
- [45] Y. Tsai, L. Zheng, and X. Wang, "Millimeter-wave beamformed full-dimensional MIMO channel estimation based on atomic norm minimization," *IEEE Trans. Commun.*, vol. 66, no. 12, pp. 6150–6163, 2018.
- [46] S. Noh, M. D. Zoltowski, Y. Sung, and D. J. Love, "Pilot beam pattern design for channel estimation in massive MIMO systems," *IEEE J. Sel. Topics Signal Process.*, vol. 8, no. 5, pp. 787–801, 2014.
- [47] B. Böck, M. Baur, V. Rizzello, and W. Utschick, "Variational inference aided estimation of time varying channels," in *IEEE Int. Conf. Acoust., Speech Signal Process. (ICASSP)*, 2023, pp. 1–5.
- [48] K. Schäcke, "On the Kronecker product," *Master's thesis, University of Waterloo*, 2004.
- [49] K. B. Petersen, M. S. Pedersen *et al.*, "The matrix cookbook," *Technical University of Denmark*, vol. 7, no. 15, 2008.
- [50] C. F. V. Loan, "The ubiquitous Kronecker product," *J. Comput. Appl. Math.*, vol. 123, no. 1, pp. 85–100, 2000.
- [51] S. Boyd and L. Vandenberghe, *Convex Optimization*. Cambridge University Press, 2004.
- [52] R. A. Horn and C. R. Johnson, *Matrix Analysis*. Cambridge University Press, 2012.